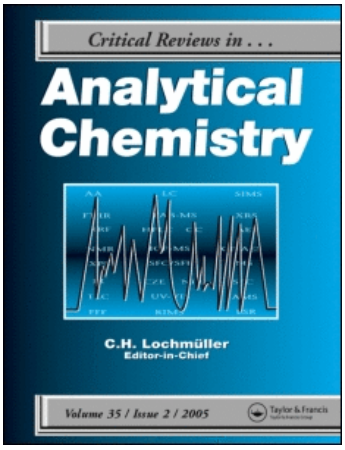

Critical Reviews in Analytical Chemistry
Publication details, including instructions for authors and subscription information:
http://www.informaworld.com/smpp/title~content=t713400837

Chemometric Techniques in Electrochemistry: A Critical Review

Steven D. Brown[a]; Robert S. BearJr Jr[a]
[a] Department of Chemistry and Biochemistry, University of Delaware, Newark, DE

To cite this Article Brown, Steven D. and BearJr Jr, Robert S.(1993) 'Chemometric Techniques in Electrochemistry: A Critical Review', Critical Reviews in Analytical Chemistry, 24: 2, 99 — 131
To link to this Article: DOI: 10.1080/10408349308048820
URL: http://dx.doi.org/10.1080/10408349308048820

Critical Reviews in Analytical Chemistry, 24(2):99–131 (1993)

Chemometric Techniques in Electrochemistry: A Critical Review

Steven D. Brown and Robert S. Bear, Jr.*

Department of Chemistry and Biochemistry, University of Delaware, Newark, DE 19716

Referee: Stanley N. Deming, Department of Chemistry, University of Houston, Houston, TX.

* Author to whom correspondence should be addressed

ABSTRACT: With the ever-increasing power and low prices of modern laboratory microcomputers it is becoming common for the average researcher to routinely employ sophisticated data analysis methods. Most of these methods have been the subject of study by researchers associated with the discipline of analytical chemistry known as chemometrics. Although the application of chemometrics has become routine in all fields of analytical chemistry, this article is focused on those applications appearing in electroanalytical chemistry. Examples of chemometric solutions to a variety of electrochemical problems are reviewed in conjunction with brief presentations of the relevant chemometric background.

KEY WORDS: chemometrics, electrochemistry, data analysis, parameter estimation, pattern recognition, calibration.

I. INTRODUCTION

Chemometrics is the discipline of analytical chemistry concerned with the application of statistics, mathematics, and other methods of formal logic to the generation and analysis of chemical data. In this article the role of chemometrics in electroanalytical chemistry will be reviewed. As in other areas of analytical chemistry, researchers are increasingly turning to chemometric methods to extract more information from their data, solving electrochemical problems that have not been approached by more conventional methods. For example, the resolution of overlapping responses, a problem that has long plagued the experimentalists, can be readily solved by any of a variety of chemometric techniques. Although this is but one application, the examination of almost any kind of electrochemical data can benefit from the application of chemometric techniques and principles.

Routine application of chemometric methods abounds in the literature of analytical chemistry, but only a small fraction of this literature has been devoted to the field of electrochemistry. Although the number of groups employing chemometric methods in electrochemistry has been limited, there has been some good progress made by them. Some of this progress has been reviewed previously. A review of chemometrics in ion-selective electrode potentiometry[1] and a very brief discussion covering chemometric principles in electrochemical analysis[2] have appeared previously. The scope of these reviews is limited, and a more general review of chemometrics in electroanalytical chemistry is attempted here. With this in mind, the purpose of this review is twofold: first, we attempt to give a brief overview of a selection of chemometric methods used in the field of

1040-8347/93/$.50

electroanalytical chemistry; second, with each method a short introduction is given to illustrate the mechanics of these techniques. Most readers will find that minimal background in chemometrics is required because the salient points of each method are presented within. More advanced coverage of the basic chemometric and numerical methods discussed here is available in a number of texts.[3,4]

This review is not intended to be comprehensive. Instead, only a small selection of papers is used to illustrate the different methods. Additionally, the weighting of individual topics within the review was chosen to reflect the author's research interests. We apologize in advance that not every paper could be cited, but we feel that our approach is better able to introduce the field and invite other researchers to improve their skills in data analysis.

II. MULTIVARIATE ANALYSIS AND CALIBRATION

One of the primary concerns in analytical electrochemistry, as in all of analytical chemistry, is modeling the output of a sensor or set of sensors as a function of changes in analyte concentrations. This type of modeling is termed calibration. The calibration relation that is established through modeling of the response-concentration relationship is used to predict the concentration of an unknown from its measured response. Although all chemists have encountered simple univariate calibration — one which considers only one independent and one dependent variable — few are familiar with the methods of multivariate analysis and calibration. Multivariate calibration extends the basic ideas of modeling and prediction that are used in univariate calibration to several independent and dependent variables. It is not uncommon to have spectra or other measured responses consisting of hundreds of independent variables and dependent variables with five or ten concentrations involved in a single multivariate calibration.

In the ensuing discussion the following notational conventions will be used: A scalar quantity will be denoted by a lowercase letter (a). Column vectors will be represented by bold, lowercase letters ($\mathbf{a}$), row vectors will be presented as the transpose of a column vector ($\mathbf{a}^T$), and matrices will be indicated by bold, uppercase letters ($\mathbf{A}$). Elements of vectors and matrices will be presented as the corresponding lower- or uppercase letters in Italic type, with the appropriate indices shown as subscripts (A_{jk}).

A. Calibration by Use of Multiple Linear Regression

When many independent variables are involved in a calibration model, and these variables are linearly related to a set of dependent variables, the simplest and most direct mathematical model relating the independent and dependent variables is found by use of multiple linear regression (MLR). In MLR, each of the dependent variables (here, the response r), is expressed in terms of a linear combination of the set of independent variables (the set of n concentrations c_i)

$$r = \sum_{i=0}^{n} b_i c_i + \mathrm{f} \qquad (1)$$

where b_i are a set of regression coefficients and f is an error term. When multiple measured responses are present, the following set of simultaneous equations, represented in matrix notation, are generated:

$$\mathbf{r} = \mathbf{Cb} + \mathbf{f} \qquad (2)$$

If more than one dependent variable is present, Eq. (2) can be generalized as

$$\mathbf{R} = \mathbf{CB} + \mathbf{F} \qquad (3)$$

The model defined in Eq. (3) is known in the statistics and chemometrics literature as the classical model. For a given set of independent and dependent variables, the goal of calibration is the estimation of the matrix of regression coefficients ($\mathbf{B}$), which define the MLR model. These coefficients are obtained by minimizing the summed, squared differ-

ence between the model Eq. (3) and the data, giving the "classical least-squares" solution

$$\mathbf{B} = (\mathbf{C}^T\mathbf{C})^{-1}\mathbf{C}^T\mathbf{R} \qquad (4)$$

The least-squares method for finding the coefficients works very well when the independent variables are either orthogonal or very close to it. Correlation between the independent variables can lead to problems in the estimation of the regression coefficients (**B**). This results from the inversion of a matrix ($\mathbf{C}^T\mathbf{C}$) with a large condition number. Fortunately, it is possible to avoid problems with MLR by taking care in measuring the mixtures, often by making the mixtures with the aid of an experimental design.

A few examples of calibrations using MLR have appeared in the electrochemical literature for analyzing voltammetric and polarographic data. Turnes et al.[5] have applied MLR to resolve highly overlapped peaks produced by differential pulse polarography and anodic-stripping voltammetry. The method of standard additions was employed to generate the calibration data. Although the authors reported good results when using MLR on differential-pulse polarography data, MLR analysis of data obtained by anodic-stripping voltammetry did not yield the same level of performance. The authors reported that slight shifts in peak positions observed in the anodic-stripping voltammograms contributed to the less satisfactory results.

Multicomponent analysis was demonstrated for ion-selective electrode arrays by Beebe et al.[6] Their work extended earlier studies conducted by Otto and Thomas[7] that focused on the application of multivariate calibration based on partial least-squares regression, a technique discussed elsewhere in this review. In both of these studies, the first step in developing a procedure suitable for the application of linear calibration methods was the linearization of the extended Nernst, or Nicholski, equation

$$E_{ij} = E_j^0 + S_j \log\left(a_{ik} + \sum_{l=1}^{N} K_{jkl}a_{il}\right) \qquad (5)$$

where the potential, E_{ij}, is measured for the ith sample at electrode j, E_j^0 is the formal potential for the jth electrode, S_j is the measured slope for the electrode in the absence of interferents, K_{jkl} is the selectivity coefficient for the kth analyte at the jth electrode with interfering ion l, and a_{ik} is the activity of the kth analyte in the ith sample.

Beebe and co-workers[6] employed a simplex optimization scheme to estimate the nonlinear selectivity parameters for each electrode. These values were then used in a MLR for the estimation of unknown concentrations. Once the estimation is performed, the analysis of unknown samples proceeds by a straightforward linear prediction step. Because this approach uses the simplex optimization to estimate the selectivity coefficients directly from the multicomponent samples, these need not be determined through separate calibrations for the individual electrodes. This is a distinct advantage in that the experimental aspects of calibrating the array are simplified. Other methods for handling this problem are subsequently discussed in their respective sections.

The *nonlinear* aspects of calibration of ion-selective electrodes and the problems associated with the application of simple, linear calibration methods are more typical of the electrochemical literature on ion-selective electrodes. The detection limit in ion-selective membrane-electrode calibrations was discussed in one article.[8] The authors suggested that the true detection limits were much smaller than those obtained using a simple linear calibration and that consideration should be given to the nonlinear response characteristics of these electrodes. Liteanu et al.[9] discussed the selectivity of ion-selective membrane electrodes, based on a statistical analysis of the effects of interferent species. Nonlinear calibration of ion-selective electrodes was demonstrated by Jain and Schultz,[10] who used a Levenberg-Marquardt nonlinear least-squares regression method to obtain the calibration parameters. In each of these studies, the authors claimed benefits such as enhanced performance and an extended calibration range as

a result of considering the nonlinear aspects of ion-selective electrode calibrations.

B. Calibration by Use of Kalman Filtering

For some problems in electrochemistry, there might be an advantage to performing MLR recursively, one dependent variable at a time, rather than all at once in a "batch" calculation. Recursive estimation methods, such as the Kalman filter, offer many advantages over the more common batch processing calculations based on MLR. The most important of these is that recursive algorithms do not require that all of the data be available for analysis; therefore, real-time calibration is possible. Additionally, recursive methods can also be applied to off-line data analysis. This flexibility does not come at the cost of accuracy, because the linear Kalman filter will perform at least as well as MLR methods relying on batch calculations. There is only a slight difference in the speed of calculations. Full details concerning the Kalman filter and the filter algorithm can be found elsewhere.[11]

Using the Kalman filter requires a different approach to the regression than that used with a batch regression method. Generally, the problem to be solved is formulated in state-space notation. The data must be measured at discrete intervals, indexed in time, potential, or other relevant variable. For consistency throughout this paper the data are considered to be sampled as a function of time, unless otherwise noted. In this approach the desired calibration parameters are estimated as elements of the state vector, which is a set of adjustable parameters to be estimated from the input data. The Kalman filter algorithm consists of a sequence of projection and update steps that are repeated for the data at each time increment. Values for the state vector and its associated error (stored as a covariance matrix) are projected for the present time increment. These estimates are based only on the values present at the previous time increment and the system dynamics, which describe the time-dependent characteristics of the system model. From the estimated state vector, a predicted system response is calculated. The response predicted for the present time increment is then compared to the measured value and a weighted correction to the state vector is made, where the weighting coefficients are known as the Kalman gain matrix. By repeating these steps, the regression is performed in a recursive manner with the present value of the state vector being a weighted combination of the estimates based on present and all previous data.

The Kalman filter also differs from typical "batch" methods based on MLR in that the Kalman filter makes use of two models. The system model describes the deterministic and random changes that occur in the states with each time step. The measurement model describes the mathematical relationship between the state vector and the measured responses at each time step. A linear measurement model, defining the system's response as the product of the measurement response matrix and the state vector, is typically used for multicomponent analysis. In this section only the linear, discrete Kalman filter and its applications to multicomponent calibration and prediction will be discussed. Electrochemical studies making use of Kalman filters with nonlinear measurement models and smoothing methods based on the Kalman filter will be presented in later sections.

Seelig and Blount[12] first used the Kalman filter in a theoretical study that considered the possibility of quantitating single analytes from anodic-stripping voltammograms. In this study, the authors used two separate filter configurations to estimate the concentration of a single component. The first configuration of the Kalman filter involved a single-measurement, single-state filter where the measured current was used to estimate the analyte concentration. The second configuration employed was a two-measurement, five-state Kalman filter where both the potential and current measurements were input to the filter for the estimation of the analyte concentration, the applied potential, current background slope, current background intercept, and the slew rate. Both of these filter

configurations were based on the incorporation of a theoretical current response function as the measurement model. Further studies[13,14] by Seelig and Blount extended their work to experimental data taken at both the hanging mercury drop electrode and the thin film mercury electrode. Their studies compared the performance of the pseudo-real-time Kalman filter method — the data were recursively filtered off-line after the actual data collection — to non-real-time or batch-regression analysis based on MLR. Results of the Kalman filtering were always in excellent agreement with those produced by the batch method. Additional studies revealed that the correlation between the true analyte concentration and the recursively estimated value was very high well before the filter reached the peak current in the voltammogram. This rapid convergence observed in the concentration estimates demonstrated that quantitation with the Kalman filter method had greater possibilities for dynamic control than would be possible with batch regression methods.

In addition to single-component quantitation, the Kalman filter has also been applied to problems in multicomponent analysis. Brown and Brown[15] demonstrated the application of the Kalman filter to the resolution of an overlapped-multicomponent linear sweep voltammogram. In this work the authors used a filter with a single input measurement, the current, and a filter state vector consisting of the concentrations to be estimated. The other fundamental difference in this work from that of Blount and Seelig was the use of the experimental, single-component voltammograms in the measurement-observation matrix. This feature allows the filtering method to be extended to systems where no theoretical model for the response current exists. Using synthetic studies, the authors demonstrated that, given sufficient signal-to-noise ratio and density of data points, overlapped voltammograms with peak separations as little as 2.5 mV (two points difference) could be resolved with the filter. The method was then applied to experimental data for the two- and three-component mixtures, Cd(II)/In(III) and Cd(II)/In(III)/Pb(II). With peak separations of from 40 to 200 mV, these overlapped voltammetric responses were well resolved by filtering. Due to the high resolving power of the filter-based analysis, small experimental peak shifts observed for the components present in the mixtures limited the accuracy of the results. The other major limitation was the use of one-point calibration for each of the components. Although the calibration for Cd(II), In(III), and Pb(II) showed strictly linear relations between response and concentration (r^2 was usually better than 0.999), small fluctuations in the estimated slope of the calibration line also had an effect on the accuracy of the results. In Figure 1 the results of the resolution of an overlapped, two-component system are displayed. The Kalman filter used for this analysis was modified to allow for small shifts in the peak potential. The approach used in this study was later extended[16] to the analysis of overlapped square-wave voltammograms of severely overlapped responses from Tl(I) and Pb(II). The ratio of concentrations of Pb:Tl was varied from 50:1 to 1:60. In mixtures where Tl(I) was the major component, errors for the estimation of the concentrations were reported to be about 1%, but slightly larger errors (2 to 5%) were obtained for the mixtures with Pb as the major component. Additional experiments performed in this work included Cd(II) as an unmodeled component in the mixtures, demonstrating the robust character of the quantitation using the Kalman filter.

C. Methods Based on Soft Modeling

Soft modeling of data involves the identification of a model *from* a data set, rather than the fitting of an external model *to* the data set. Generally, the variation caused by some extended, systematic changes in the system producing the data are the target of a soft modeling study. Probably the most common chemometric method used for soft modeling is principal components analysis (PCA), a family of computational techniques concerned with the isolation of the sources of

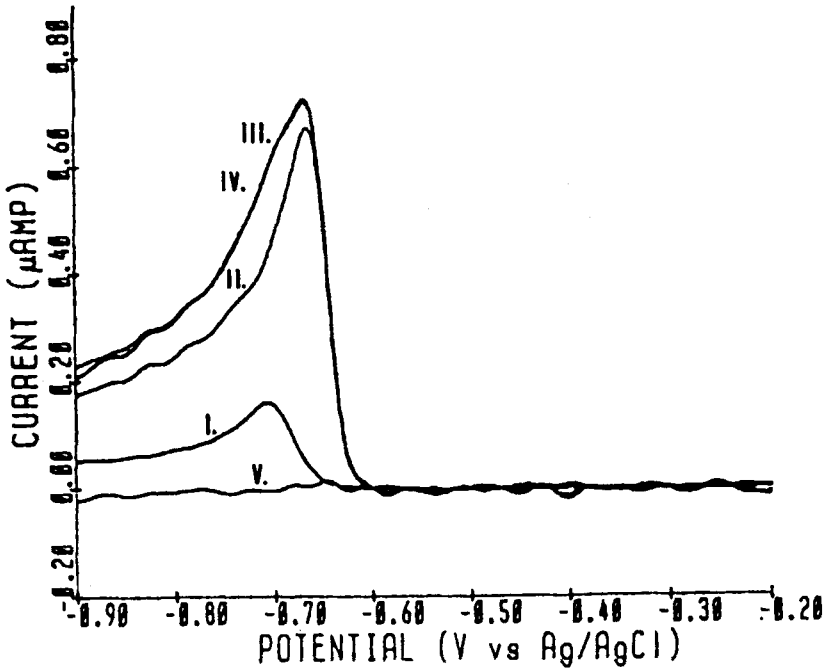

FIGURE 1. Peak separation of a two-component Cd(II) / In(III) system: (I) Cd(II) wave; (II) In(III) wave; (III) sum of Cd(II) and In(III) waves; (IV) the original voltammogram; (V) the residuals of the fit (also called the innovations sequence). (Reproduced from Brown, T. F.; Brown, S. D. *Anal. Chem.* **1981**, *53*, 1410–1417. With permission from The American Chemical Society.)

variation in a data set. Several texts[3,17-19] discuss the different aspects of this subject in considerable detail, and only a brief overview will be provided in this review. The sources are isolated by a decomposition of the data set into its eigenvalues and eigenvectors, as outlined in the following equations.

The initial step in principal components analysis is the formation of the data covariance matrix, given as

$$\mathbf{Z} = \mathbf{D}^{\mathrm{T}}\mathbf{D} \tag{6}$$

where **Z** is the covariance matrix and **D** is the original data matrix. The covariance matrix, **Z**, is then diagonalized through a unitary transformation

$$\mathbf{\Lambda} = \mathbf{V}^{-1}\mathbf{Z}\mathbf{V} \tag{7}$$

where $\mathbf{\Lambda}$ is a diagonal matrix whose elements are the eigenvalues of **Z**, and **V** is the matrix of eigenvectors, often referred to as abstract factors or as the loadings. These loadings are the projections of the data onto an orthonormal basis set spanning the data in **D**. That basis set is defined by the data scores, **T**. Collectively, the scores and loadings are called the principal components of the data. Some authors call them factors of the data. The data in **D** can be reproduced from the loadings and scores by the relation

$$\mathbf{D} = \mathbf{T}\mathbf{V}^{\mathrm{T}} \tag{8}$$

A convenient method, which has become standard for performing the eigenanalysis in Eq. (7), is by a singular value decomposition. This eigendecomposition method is now available as part of most numerical analysis software. In singular value decomposition the data matrix is decomposed into the product

of three matrices:

$$\mathbf{D} = \mathbf{USV}^T \quad (9)$$

where **U** is a matrix of the row eigenvectors (eigenvectors of $\mathbf{DD}^T$), **S** is a diagonal matrix of the singular values (the square roots of the eigenvalues), and **V** is a matrix of the column eigenvectors (eigenvectors of $\mathbf{D}^T\mathbf{D}$). The eigenvector matrix, **V**, obtained by singular value decomposition, is equivalent to the matrix **V** of Eq. (7). The matrix product of the row eigenvector matrix **U** and the singular values matrix **S** is equivalent to the scores matrix **T** in Eq. (8).

Noise reduction in the data is one benefit that often results from this decomposition process. Given that n measurements were used in the data set, **D**, there will be n eigenvectors produced in the diagonalization Eq. (7). Not all of the eigenvectors produced convey useful information; some represent mostly noise components of the data set. When the data have been properly collected, with high signal-to-noise-ratio, the noise will dominate in those eigenvectors with small eigenvalues because the noise contributes only a small amount of the total variation in the data. Removal of those loadings associated with small eigenvalues does not hinder reconstruction of the information present in the original data matrix, and a noise reduction results from using the truncated loadings and scores in Eq. (8). In cases where noise is a significant part of the data, however, the correct number of factors to retain may not be readily apparent. By careful selection of a subset of the eigenvectors, keeping eigenvectors containing mostly "signal" and dropping those containing mostly "noise" from the analysis, it is possible to reduce noise in a data set. The data usually can be represented in a space containing a lower number of dimensions. Other benefits, such as determining the true underlying dimensionality of a problem, are also obtained by this decomposition. It is often possible to reduce a data set collected over hundreds of independent variables to only a few nonnoise eigenvectors by means of a PCA. The reduced dimension and high information content of the principal components often simplifies subsequent data analysis.

Despite its importance to the field of data analysis and its common use in spectroscopy and elsewhere, very few examples of methods based on PCA have been reported in the electrochemical literature. This lack of interest by electrochemists is unusual given the ready acceptance of these methods in other areas of analytical chemistry. It is interesting to note, however, that one of the first applications of PCA was reported in electrochemistry, over 2 decades ago. Early work by Howery[20] reported on the use of PCA to study polarographic half-wave potentials of alkaline and alkaline-earth metal ions in five separate polarographic solvents. Although this study was brief, the issue of determining the appropriate number of factors required to describe the solvent-caused variation in the data was addressed. Howery found that three principal components were required to adequately model the half-wave potentials in each of the solvent systems. Once the PCA model was built, physically significant ion and solution parameters, such as the ionic charge, the ionic potential, and the solvent's molar enthalpy of vaporization, were then treated as new dependent variables, and a MLR model was built from the three principal components and these physical measurements. A low prediction error in this modeling — known as target testing — indicates that the test vector made from the dependent variables can be rotated onto the space spanned by the principal components. This result means that the parameters being tested are consistent with the source of variation present in the data, and that it *might* be possible to predict these properties from the electrochemical responses.

Principal components analysis can also be used to estimate the number of components present in a system when the number of systematically varying physical components is not known. If the data vectors that represent sample responses are recorded at regular, discrete increments of time, potential, or some other indexing variable, the

evolution of the number of components present in the mixture can be assessed as a function of the indexing variable. A technique known as evolving factor analysis (EFA) is one method for performing this type of estimation.[17,21] Evolving factor analysis is performed by starting at one end of a data set and defining a subset of the data, composed of the first few sample response vectors. Principal components analysis is then performed and the eigenvalues obtained are recorded. A new subset is then defined by adding one more sample response vector to the previous matrix and PCA is performed again. This process is repeated until the subset includes all of the original data matrix. This completes the "forward scan". The process of generating subsets, eigendecomposing, then adding another sample, and repeating the eigendecomposition is then done starting at the other end of the data and working in the opposite direction — a "backward" scan. Plotting the largest few eigenvalues for each factor in the forward and backward scans as a function of the indexing variables gives information on the regions of the data where changes in systematic response occur — perhaps due to changes in the ratios of overlapped components.

Evolutionary factor analysis was used by Kankare et al.,[22] who studied the spectroelectrochemical data produced from cyclic voltammetry of poly(3-methylthiophene) in 0.1 *M* tetrabutylammonium perchlorate in acetonitrile solvent. Rather than plotting the individual eigenvalues directly, the authors plotted the residual standard deviations obtained for the largest eigenvalues in each of the decompositions. The residual standard deviation, which is a measure of the unexplained variation remaining in the data set, is given as

$$s_k = \left(\frac{\mathrm{tr}(\mathbf{Z}) - \sum_{i=1}^{k} \lambda_i}{n_w - k} \right) \qquad (10)$$

where k is the number of the eigenvalue, tr(**Z**) denotes the trace of the data covariance matrix, and n_w is the number of response variables present in the data set. Figure 2 shows the residual standard deviations for the first three eigenvalues produced from spectra obtained during the forward (s_k) and backward ($\bar{s}_k$) EFA of the data for the anodic sweep of the voltammogram. In each direction, as the number of factors required to describe the variation in the spectral data increases, so do the residual standard deviations of those eigenvalues corresponding to factors that number less than the number of components. The results produced by the foregoing standard evolving factor analysis were also compared to those of differential evolutionary factor analysis. In differential EFA, the size of the data subset used in the decompositions remains constant, but the window of sample response vectors is incremented through the original data matrix. The size of this window is critical to the analysis. A window that spans too broad a region in time will lower the resolving power of the method, and windows containing too few spectra may be subject to statistical variations. Figure 3 shows the results of applying differential EFA to the same spectral data set used to produce Figure 2. A peak-shaped response results from eigendecomposing the data using a moving window, making the formation of new components more readily identifiable. With the aid of both of these eigendecomposition approaches, Kankare and co-workers were able to clearly identify the presence of transient species produced during the cyclic voltammetric run.

A third technique employed by Kankare et al. was based on a projection matrix that enables the influence of individual component spectra to be removed from the data. If Beer's law holds, each of the spectra in the data matrix is comprised of the sum of the spectra for all components present in the sample, which is given as

$$\mathbf{a}_j = \sum_{i=1}^{N} X_{ij}\mathbf{s}_i \qquad (11)$$

where $\mathbf{a}_j$ is the measured spectrum for sample j, X_{ij} is the mole fraction of component i

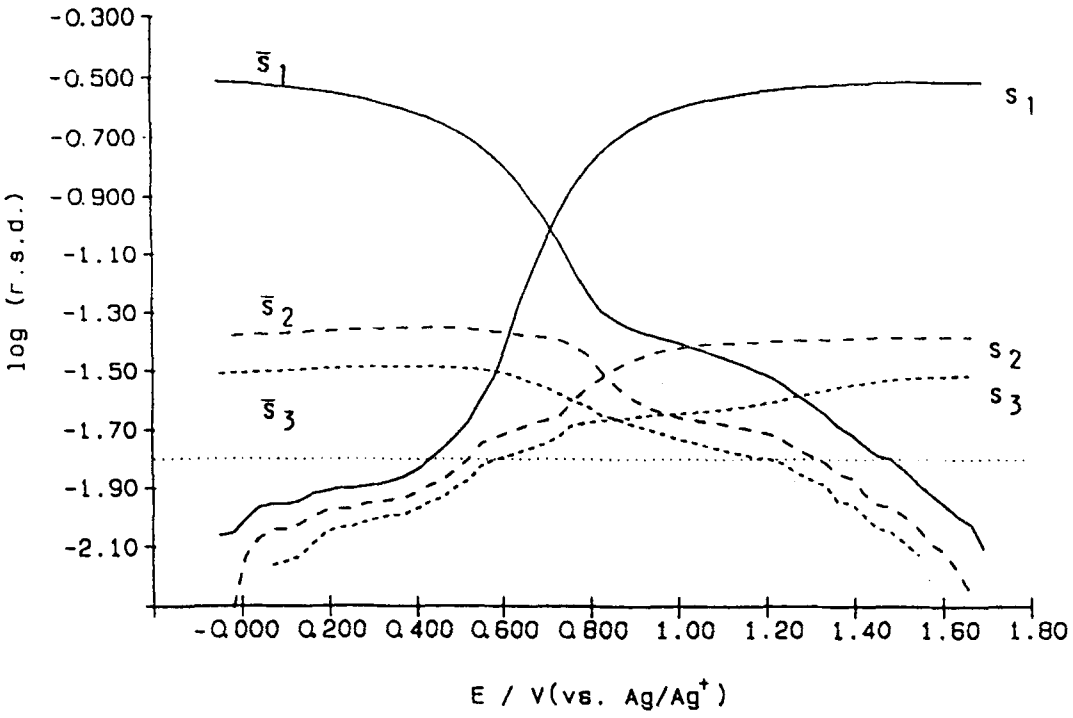

FIGURE 2. Evolving factor analysis of the spectra recorded during the anodic sweep of a cyclic voltammetric measurement. The standard deviation of the absorbance measurements is shown by the horizontal dotted line. (Reproduced from Kankare, J.; Lukkari, J.; Pajunen, T.; Ahonen, J. *J. Electroanal. Chem.* **1990**, *294*, 59–72. With permission from Elsevier Sequoia S.A.)

in sample j, and $\mathbf{s}_i$ is the spectrum of component i. The projection matrix for removing the mth component is

$$\mathbf{P} = \mathbf{I} - \frac{\mathbf{s}_m \mathbf{s}_m^T}{\mathbf{s}_m^T \mathbf{s}_m} \tag{12}$$

where $\mathbf{I}$ is the identity matrix. Multiplying spectrum $\mathbf{a}_j$ by the projection matrix yields

$$\mathbf{Pa}_j^T = \sum_{i \neq m}^{N} X_{ij} \mathbf{Ps}_i \tag{13}$$

Note that Eq. (13) describes another MLR model with dependent variable $\mathbf{Pa}_j^T$ and independent variables $\mathbf{Ps}_i$. To generate a projection matrix, the spectra of the components to be removed from the data must be known. The amount to remove is determined from Eq. (13). Thus, the projection matrix provides one approach to quantitative removal of known components in unknown mixtures by MLR. It can be considered as a complement to the target testing of data, a technique used to identify the presence of a test vector in the data, which is also based on MLR.[17]

Using the projection matrix, the authors analyzed the time-dependent spectral data produced during a potential-step experiment on the poly(3-methylthiophene) system. Based on the supposition that the oxidation of the analyte followed a consecutive reaction scheme, where A → B → C, the principal components corresponding to the initial and final species were selectively removed from the spectral data. The resulting spectral data clearly displayed the time-dependent evolution and consumption of an intermediate species. This work illustrates the potential of PCA as a means for extracting more information from electrochemical data than is available by the more conventional methods presently in use.

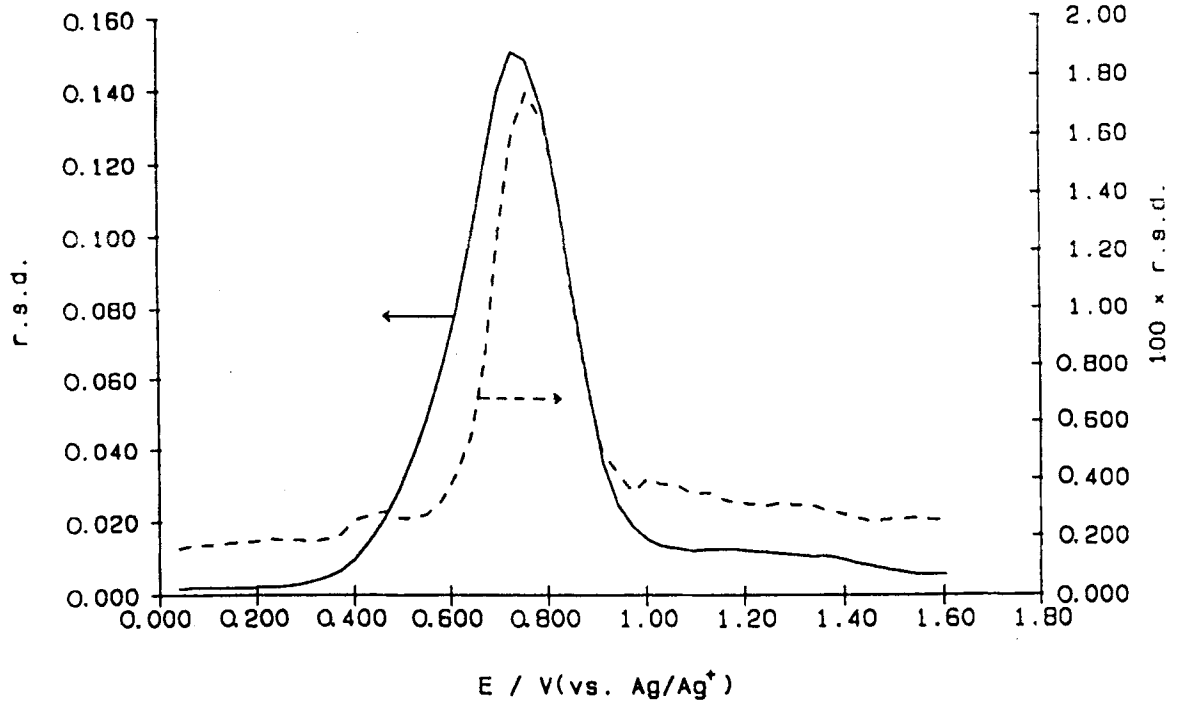

FIGURE 3. Differential evolving factor analysis of the spectra obtained during the anodic sweep of a cyclic voltammetric measurement. Solid curve: more than one component; dashed curve: more than two components. (Reproduced from Kankare, J.; Lukkari, J.; Pajunen, T.; Ahonen, J. *J. Electroanal. Chem.* **1990**, *294*, 59–72. With permission from Elsevier Sequoia S.A.)

Principal components analysis has other uses in quantitative analysis of data. For example, representing a data set by a reduced number of orthogonal variables has tremendous mathematical advantages when a regression is to be performed. Careful truncation of the scores and loadings of a data set with low noise content permits modeling of only the systematic variation, and not the noise. This combination of MLR and PCA, known as principal components regression (PCR), has many useful applications. The key step in obtaining a successful regression using principal components as the set of independent variables involves the removal (by truncation) of nonsignificant scores and loadings from the data. When an incomplete set of scores and loadings are used to represent a data matrix **D**,

$$\hat{\mathbf{D}} = \bar{\mathbf{U}}\bar{\mathbf{V}}^{\mathrm{T}} \qquad (14)$$

an estimated data matrix $\hat{\mathbf{D}}$ results. In Eq. (14), $\bar{\mathbf{U}}$ and $\bar{\mathbf{V}}$ are the truncated scores and loadings matrices. Because a reduced number of principal components is used in the reconstruction, the information present in the original data has been compressed to a space of lower dimension. In addition to this compression, the new variables used to represent the data are orthogonal, because they are scores.

This is the basis of PCR, a form of MLR that relates a dependent variable **Y** to a set of independent variables in **D** by using a truncated scores matrix obtained from **D** in place of the original independent variables in **D**:

$$\mathbf{Y} = \bar{\mathbf{U}}\mathbf{B} \qquad (15)$$

Estimation of the regression coefficients is performed by least-squares regression, just as

in MLR, but with the important advantage that the inversion of $\bar{\mathbf{U}}^{\mathrm{T}}\bar{\mathbf{U}}$ proceeds without difficulty.[18] Modeling with PCR offers the possibility of including highly correlated independent variables, such as spectra or voltammograms, in the model without any worry that the matrix inversion shown in Eq. (4) may fail due to the high degree of similarity of the independent variable. It also permits the use of an inverse model, where the response matrix **R** is modeled as the independent variable, and the concentration matrix **C** is treated as the dependent variable:

$$\mathbf{C} = \mathbf{RB} + \mathbf{F} \tag{16}$$

Note that the inverse model presumes that all error is carried in the concentration. This assumption is unusual, but it can be satisfied if proper truncation of the score of **R** is done and if $\bar{\mathbf{U}}$, the truncated scores of **R**, are used in the regression model, giving the relation

$$\mathbf{C} = \bar{\mathbf{U}}\mathbf{B} \tag{17}$$

Fitting Eq. (17) to the scores of data has the double advantage of requiring fewer independent variables and using data with less noise because of the data compression and noise reduction generated in eigendecomposition and the truncation of the response data in **R**. With these benefits comes a pitfall for the unwary: care must be taken to select a *suitable* truncation, one where little useful information is removed from the data. Improper truncation will cause errors in the modeling as a result of the introduction of a bias, and that bias may not be readily apparent to the uninitiated user. Methods for selecting the proper truncation have been discussed.[18]

Partial least-squares (PLS) regression extends the idea of using the inverse model and replacing variables with a truncated set of their principal components.[18] In PLS regression, both the independent variables (called the **X** block) and dependent variables (called the **Y** block) are eigendecomposed simultaneously. The PLS "outer relations" equations, which define the eigendecomposition of the **X** and **Y** matrices, have the same form as PCR:

$$\mathbf{X} = \mathbf{TP}^{\mathrm{T}} + \Omega = \sum t_h p_h^{\mathrm{T}} + \Omega \tag{18}$$

$$\mathbf{Y} = \mathbf{UQ}^{\mathrm{T}} + \mathbf{F} = \sum u_h q_h^{\mathrm{T}} + \mathbf{F} \tag{19}$$

where **T** and **U** are the scores for the two blocks, **P** and **Q** are the respective loadings, and Ω and **F** are residual matrices made from the scores and loadings of the discarded principal components. The simultaneous decomposition of the **X** and **Y** blocks is controlled by the "inner relation"

$$\hat{u}_h = b_h t_h \tag{20}$$

where b_h is the vector of regression coefficients for the hth principal component in the **X** and the **Y** block. This inner relationship essentially determines the rotation of the **X** and **Y** data to maximize the correlation between the two blocks.

Many types of electrochemical experiments produce quantitative data suitable for modeling with PCR or PLS regression. Surprisingly, few applications have appeared. One application has been reported by Henrion et al.,[23] who used PLS regression to quantitatively resolve overlapping responses obtained from differential-pulse anodic-stripping voltammetry. In this work, the authors demonstrated that a calibration developed from a rather small data set with the aid of PLS regression gave results for a two-component problem that were superior to those obtained by a vastly simpler analysis using only the measured current at two potentials to solve simultaneous equations for the concentrations.

Data that are not directly suitable for these soft modeling and calibration methods can often be transformed prior to the analysis. As previously discussed, the extended Nernst (Nicholski) equation, used in the calibration of ion-selective electrodes, is nonlin-

ear and therefore not directly amenable to linear calibration methods. Otto and Thomas[7] have applied PLS regression to develop a calibration model for an array of ion-selective electrodes used in the simultaneous determination of Ca^{2+}, Mg^{2+}, K^+, and Na^+. The authors found that calibration using PLS modeling produced lower prediction errors than MLR; the disparity between the methods was observed to increase as more ion-selective electrodes were included in the sensor array. When more electrodes are used in the array, more redundant information is present in the set of sensor responses for each sample. This correlation between the response variables can lead to a degradation of the performance observed for MLR, as discussed before. In contrast, the performance of the PLS calibration should not be affected by the collinearity in the sensor outputs because the regression is better conditioned. In calibrations where a large number of correlated independent variables are used, the application of PLS regression can provide performance significantly better than that of MLR.

D. Projection-Pursuit Regression

Occasionally, a linear relation between the independent and dependent variables cannot be forced. In these cases, a nonlinear calibration method is useful. One nonlinear calibration method that has only recently been applied in chemistry, and specifically in electroanalytical chemistry, is projection-pursuit regression. In projection-pursuit regression the response variable matrix **R** is modeled as a function of linear combinations of the independent variables, for example, concentration. The function used is an empirically determined smoother

$$\mathbf{r}_j = G_j\left(\sum_{k=1}^{K} \theta_{kj}\mathbf{c}_k\right) + \mathrm{f}_j \qquad (21)$$

where $\mathbf{r}_j$ is a vector from the response block, G_j are the univariate smoothing functions, θ_{kj} are the regression coefficients, $\mathbf{c}_k$ is the concentration vector for the kth species, and f_j is the error associated with fitting the response for the jth sensor. This empirically determined smoother can either be used directly in the regression or replaced by an appropriate analytic function. Projection-pursuit regression offers a big advantage when dealing with complex data in that it requires no prior knowledge of the data or the underlying physical model, but it can use the analytic expression for the physical model if it is known or can be guessed.

The projection-pursuit regression algorithm starts by selecting an initial set of predictor coefficients θ, then generates a smoother **G** for the response as a function of the selected linear combinations. From the smoothed response function, the fraction of unexplained variation in the data is determined and used to evaluate the fit. If the value of the unexplained variation contained in the fit falls below a user-defined threshold, the regression algorithm is terminated; alternatively, the preceding process can be repeated until the desired tolerance is obtained.

The most common situation where nonlinear relations between response and concentration arises is with ion-selective electrodes. As previously discussed, linearization of the nonlinear relation can be used, but there are limits to the accuracy of any linearization method. Beebe and Kowalski[24] have applied projection-pursuit regression to the multivariate calibration of ion-selective electrode arrays. The responses of the ion-selective electrodes were used as the response matrix (**R**) and the concentrations were the predictor variables (**C**). They replaced the empirical smoother with that of a logarithmic function, the theoretical response of an ion-selective electrode. The quality of the calibration produced with projection-pursuit regression did not compare favorably with that of the linearized calibration method reported by Beebe and coworkers,[6] in part because the authors used insufficient amounts of data to constrain the flexible log-linear model defined in their projection-pursuit regression. In the absence of an adequate amount of data needed to spec-

ify the form of a general, nonlinear calibration to the extent required for accurate prediction, it is often better to apply more traditional methods with a known, or assumed, underlying relation. In the case of calibration of arrays of ion-selective electrodes, linearization and subsequent calibration with MLR or PLS seems preferable to more sophisticated approaches when limited calibration data are available.

E. Artificial Neural Networks

Artificial neural networks have recently emerged as one of the fastest growing research areas in the field of chemometrics, but they have seen little use in the electrochemical literature. The interest shown by those in chemometrics and elsewhere arises from their potential applications in nonlinear mapping, in nonlinear multivariate calibration, and in linear and nonlinear pattern classification.

An artificial neural network is made from a layered array of processing units, termed neurons, that each possess multiple inputs and produce a single output. Each neuron performs two tasks: (1) taking the weighted sum of the n inputs and (2) applying a nonlinear transfer function to the weighted sum to produce the output. Typically, this nonlinear function has a sigmoidal response

$$f(x) = 1/\left(1 + \exp\left[\sum_{i=1}^{n} w_i x_i\right]\right) \quad (22)$$

where $f(x)$ represents the output of the neuron, w_i are the weights applied to the ith input, x_i is the value present at the ith input, and n is the number of inputs to this neuron.

An example of a feed-forward network, one that does not possess any signal feedback pathways connecting the output layer to another layer, is shown in Figure 4. The neurons in each layer are connected to all of the neurons present in the next layer; the ability to produce very complex nonlinear models via this interconnected topology gives the network much of its modeling power. In the figure the first layer of neurons is an input buffer, with each neuron connected to a single input.

To use an artificial neural network for calibration, a set of weights must be determined, which yield the desired set of output values when a given input pattern is applied to the network. In supervised training of the network, the network is presented with a

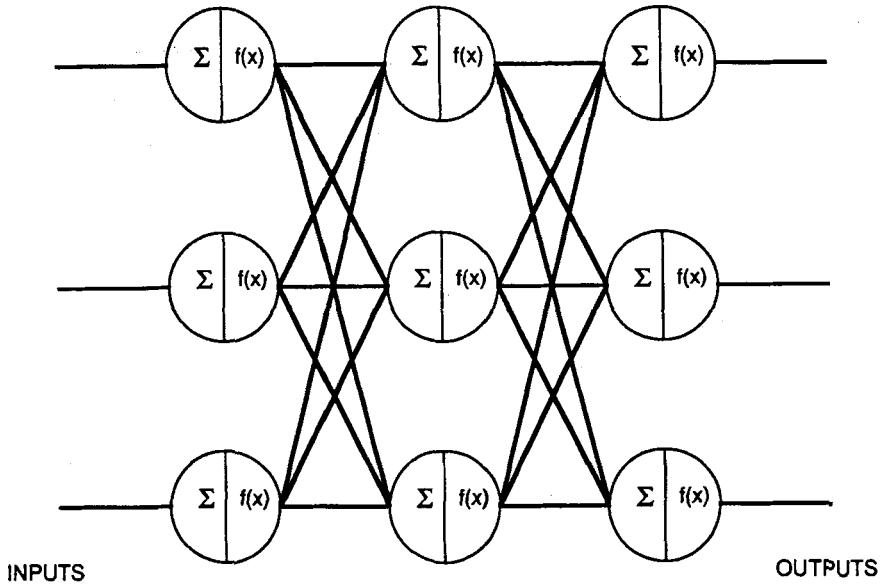

FIGURE 4. Feed-forward neural network with a single hidden layer.

series of input patterns and the resulting outputs are compared with the known reference outputs for the data in the "training set". Adjustments to the weights are made based on the error observed in the output patterns. The presentation of the input-output pairs in the training set is repeated until the outputs produced by the network match the reference patterns to within a user-specified tolerance. Some caution must be exercised in deciding when to terminate the training because the network is capable of fitting noise present on the training data when improperly trained. Although many learning algorithms have been developed for making the weight adjustments, the most popular method for training feed-forward networks is the backward error propagation rule, known in the literature of neural networks as "backprop". In backprop the global error present in the output layer is propagated backward, layer by layer, using successive applications of the chain rule for partial derivatives, until the input layer is reached. Updates to the weights are then made based on a gradient descent approach. The simplicity of the backprop algorithm makes it a convenient starting point for those interested in learning about neural networks, but its slow training can lead to very long and inefficient training sessions. Those interested in more detail on artificial neural networks might want to consult any of a number of excellent texts on the subject (for example, Reference 25).

Bos et al.[26,27] have applied neural networks to the nonlinear calibration of an array of ion-selective electrodes. They analyzed a four-component system containing Ca^{2+}, K^+, Cl^-, and NO_3^-. In addition to ion-selective electrodes for each of the ions present, the authors also included a pH electrode in the array. Because of the artificial neural network's high, nonlinear modeling power, many of the problems previously discussed in conjunction with direct multicomponent calibration of ion-selective electrode responses have been avoided. Chief among these problems was the need to separately determine the slope and selectivity coefficients; this problem becomes more complicated when the analyte ions have different formal charges. In this study, the calibration — the unknown relationship between the species concentrations and the responses produced by the electrode array — is considered to be unknown and uninteresting to the researcher. The neural network serves to provide a nonlinear mapping of the ion-selective electrode array's response for each of the calibration samples onto the known log concentration values. The precision obtained in this multivariate application was comparable to that obtained in a conventional, univariate ion-selective electrode calibration. The authors cited a mean relative error of $\pm 6\%$ in their determinations. In addition to a feed-forward network, a recurrent network with a net topology that provides a feedback pathway, was also simulated for a two-component problem involving multivariate, nonlinear calibration of Ca^{2+} and Cu^{2+}. Calibration results for the recurrent network were also similar to those obtained by linear regression with a univariate ion-selective electrode. The results of this study seem quite promising for the future of artificial neural networks in nonlinear calibration of ion-selective electrodes, but 48 h of training on a small computer was needed for the network to yield errors of a magnitude typical of ion-selective electrode measurements. The preceding linearization methods required only a small fraction of this time to generate a calibration when used to model ion-selective electrode responses.

III. PARAMETER ESTIMATION

Parameter estimation is a discipline of chemometrics concerned with fitting data to a mathematical model. It differs from calibration in that a more general model may be of interest beyond direct relations of responses and concentrations in linear or nonlinear form. Models used in parameter estimation routines can be analytic, expressible in closed form, or numerically generated. Examples of both cases are well established in the electrochemical literature. Closed-form models result either from theoretical

relations for the system under study or they can be derived empirically. Numerical models usually require extensive computations to generate the appropriate response functions. Electrochemical simulations, widely used for modeling the responses produced by complex heterogeneous and homogeneous kinetics, are an example of the types of numerical models that can be used in parameter estimation routines. Because the models used in parameter estimation are often more complex than those used in multivariate calibration, some variant of nonlinear regression is usually needed to fit the model to the data. Optimization of a set of model parameters by nonlinear regression yields a minimum in a function of the difference between the experimental and the predicted response. A wide range of nonlinear fitting methods have been reported in the electrochemical literature. These techniques range from simplex optimization to Kalman filtering and they can be applied to a wide variety of chemical models, not just those appropriate to electrochemistry. Many examples of nonlinear regression analysis in electrochemistry have been discussed in a recent review by Rusling.[28]

A. Batch Methods for Nonlinear Regression

In nonlinear regression the measured response (y) is modeled as a nonlinear function (ϕ) of the set of parameters to be estimated (Θ_i). Object functions (Ξ) to be minimized in a nonlinear regression are usually a weighted sum of the squared error between the measured and predicted responses:

$$\Xi = \sum_{j=1}^{m} w_j\left(y_j - \phi_j(\Theta_1, \Theta_2, \Theta_3, \ldots, \Theta_N)\right)^2 \tag{23}$$

where w_j are the set of weighting coefficients. In the simplest cases, all data are given equal weight (i.e., the values for the w_j are set to 1). Minimizing this object function with respect to the parameters, Θ_i, results in a nonlinear "least-squares fit" of the model h and the parameter set, Θ_i, to the data.

In nonlinear estimation, an analytic solution for the path to optimum parameters, given an exact form for the model, does not exist. Instead, the minimization of the object function is performed iteratively. These iterative optimizations can be based on either a direct search or on a gradient descent to the minimum, or, possibly for *a* minimum, depending on the presence of a single, global minimum or multiple, local minima in the error surface under study. Gradient methods require derivative information, which can be provided analytically from the model under study, or they can be numerically generated at each step in the optimization. No constraints have been placed on the solution to the problem just defined, but it is possible to modify the object function Ξ such that a constrained search for optima is performed.

Examples of nonlinear regressions based on simplex optimization, a direct search method, are commonplace in the literature of electroanalytical chemistry and of analytical chemistry as a whole. One of the better, and also earliest, examples of using the simplex-based direct search in conjunction with an explicit finite difference (EFD) simulation model was reported by Hanafey and co-workers,[29] who used EFD simulations to prepare sets of working curves for chronoamperometric, chronocoulometric, and chronoabsorptometric responses in double potential-step experiments. A series of different electrochemical mechanisms was considered and the simulations were generated to cover a wide range of kinetic behavior for each of the mechanisms. The procedure developed by the group allowed for kinetic parameter estimations to be made from reactions following known mechanistic schemes and the possible determination of the appropriate mechanism for an input data set. Parameter estimation was performed by using a simplex search, confined to two kinetic parameters, over an interpolated response surface for each mechanism. The interpolated surfaces were generated for each series of working curves corresponding to the mechanistic pathways. Although the authors sug-

gested that coupling the simulation directly to the simplex optimization would provide better estimates than were obtained with the interpolated working curves, the computation time required would have been prohibitive. As a compromise, the authors proposed using the interpolated search as an exploratory step, and refining the estimates obtained by a separate, directly coupled simulation. This approach should yield more accurate parameter estimates while making more efficient use of computer time. A similar approach, but one that did not use a simplex optimization, was proposed for the estimation of heterogeneous electron transfer kinetic parameters from asymmetric, double potential-step chronoabsorptometric data.[30] The authors employed a table lookup, based on the potential value during the second step, and interpolated working-curve surfaces to match the experimental data. Although the basic approach was the same as in the previous study, this latter work did not address the range of electrochemical mechanisms already examined. Both of these methods are based on searching a database of working curves, which eliminates the need for iterative evaluations of complex model functions. In this respect these methods reduced the overall computational burden of fitting a data set, but increased storage requirements are imposed to maintain the working-curve databases. Performing an interpolation of the working-curve surfaces helps to reduce the overall storage requirements, although at the expense of accuracy in the estimated parameters.

One of the most prominent uses of simplex-based parameter estimation in the electroanalytical literature was proposed by O'Dea et al. and later refined to what is now known as the COOL algorithm.[31-34] This method allows for the estimation of kinetic and thermodynamic parameters from pulse voltammograms of systems following an E mechanism with quasireversible kinetics. In this approach the voltammetric current is modeled by a nonlinear dimensionless current function, $\Psi(\alpha, \kappa, E^r_{1/2})$, where α is the transfer coefficient, $E^r_{1/2}$ is the reversible half-wave potential, and κ is a function of the standard heterogeneous rate constant and the diffusion constants

$$\kappa = \frac{ks}{D_O^{(1-\alpha)/2} D_R^{\alpha/2}} \tag{24}$$

Fitting the data is accomplished by performing a linear regression of the experimentally observed response against the values of Ψ provided by the nonlinear model:

$$i_{\text{observed}} = a\Psi(\alpha, \kappa, E^r_{1/2}) + b + \text{f} \tag{25}$$

where a and b are the slope and intercept of the regression line and f is the error present. A simplex search is used to find the values of α, κ, and $E^r_{1/2}$ that minimize the object function

$$S = (1 - r) \tag{26}$$

where r is the correlation coefficient of the linear regression. When the optimal values of these parameters have been obtained, the maximum correlation — largest value of r — is observed. In practice a value of $r = 1$ will not be observed due to the presence of noise in the data.

The COOL algorithm has several convenient features. Among these is the automatic scaling of the dimensionless model, removing the need for accurate measurements of the electrode area and solution concentrations. A second benefit is the compensation for instrumental offset through the estimation of the regression's intercept parameter. An additional feature of the COOL algorithm is that confidence intervals are computed by maximum likelihood for each of the estimated parameters. In principle, this method can be applied to the analysis of any pulse voltammetric response, but in practice it has seen most of its applications in square-wave voltammetry. In Figure 5 the results of fitting a series of square-wave voltammograms, collected at different frequencies, are displayed. Across the entire frequency range employed, excellent agreement was obtained between the experimental data and the fits generated by the COOL algorithm. Extensions of this method have appeared that incorporate

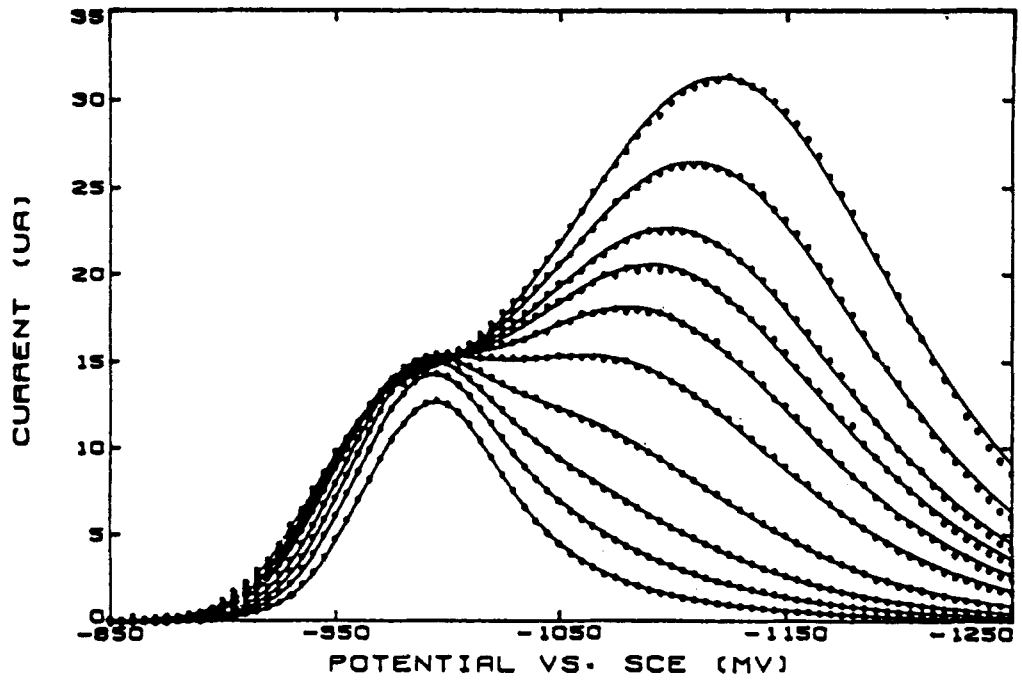

FIGURE 5. Square-wave current as a function of frequency, 1 m*M* Zn(II) in 1.05 *M* $NaNO_3$. ΔE_s = 5 mV, E_{sw} = 25 mV. Experimental (●) and theoretical (—) currents with frequencies in ascending order of curves at −1100 mV; 10, 25, 50, 100, 200, 300, 400, 500, 700, and 1000 Hz. (Reproduced from O'Dea, J. J.; Osteryoung, J.; Osteryoung, R. A. *J. Phys. Chem.* **1983**, *87*, 3911 -3918. With permission from The American Chemical Society.)

corrections for electrical double-layer effects on the observed reaction kinetics.[35]

Nonlinear regression has also been used extensively for fitting polarographic and voltammetric data. Examples range from the early work of Meites and Lampugnani,[36] to similar work reported recently for resolving overlapped polarograms.[37,38] Colina et al.[39] analyzed response surfaces produced by polarographic waves; the focus of this work was an evaluation of the precision in the resulting parameter estimates. Birke et al.[40] extracted kinetic information from differential pulse polarography by using a simplex-based nonlinear regression procedure coupled to a theoretical model for the response produced by reversible, quasireversible, and irreversible systems. By using the simplex to perform the nonlinear regression, they were able to successfully estimate the values of the heterogeneous standard rate constant, the transfer coefficient, and the reversible half-wave potential for a quasireversible system. The electrochemical system studied in this work was the reduction of Zn(II) in KNO_3 and $NaNO_3$. Results obtained in this study were in good agreement with those obtained by other methods. Fitting direct current and derivative polarograms was proposed for the analysis of first-order EC processes by Kim.[41] Experimental polarograms were fitted to a function derived for the EC mechanism. Estimates of the homogeneous rate constant and the reversible half-wave potential for the heterogeneous electron transfer reaction were obtained from the fits.

Potential-step voltammetry and semiderivative voltammetry have also been addressed by multiparameter curve fitting. Boudreau and Perone[42] used a combination of skewed Gaussian and skewed Cauchy functions to fit potential step voltammetry data. Part of this work was concerned with implementing on-line peak detection to trigger an interrupt in a staircase voltammetry experiment. The momentary pause produced in the data acquisition provides an improvement in the resolution of overlapping

responses. Toman and Brown[43] showed that semiderivative voltammetry could be treated by nonlinear regression to resolve overlapped responses for reversible systems. A three-component problem was studied with semidifferentiated linear sweep voltammetry and semidifferentiated anodic-stripping voltammetry. Components in the experimental studies could be resolved with peak separations as small as 40 mV. An extension of this work, reported by Caster et al.,[44] examined nonlinear least-squares fitting of semidifferentiated linear scan voltammograms as a function of the degree of reversibility of the electrochemical system involved. Minor changes in the semiderivative peak shapes did not significantly alter the ability to adequately fit the voltammetric data. Rusling and Connors[45] applied nonlinear regression analysis to study pseudo-first-order rate constants for electrocatalytic reactions using linear sweep voltammetry. In this application the response curves observed were of the form of a voltammetric wave so that a simple function could be used in the regressions. Results suggested that this method provided more precise parameter estimates from overlapping responses than had been obtained from a simple background subtraction.

Estimation of electrochemical kinetic parameters from chronoamperometric and chronocoulometric data using nonlinear regression and simplex searches is also well established. Rodriguez Mellado[46] used a linearization that formats the nonlinear estimation into a linear regression. This approach makes use of the same basic strategy behind the COOL algorithm. Another approach to the analysis of chronoamperometric and chronocoulometric data, one based on a multiple *linear* regression procedure, was also reported for the estimation of heterogeneous kinetic parameters.[47] Other authors have examined using nonlinear regression to fit spectroelectrochemical data produced in potential step experiments,[48] and time-dependent spectral data produced in thin layer spectroelectrochemistry experiments.[49] Chen and McCreery[50] reported fitting chronoamperometric data for the estimation of homogeneous kinetic parameters of a first-order EC mechanism. More complicated mechanistic schemes, such as an ECE mechanism, have also been addressed by nonlinear regression methods.[51] Recently, Papanastasiou et al. reported the estimation of homogeneous kinetics for an ECECE mechanism by an iterative parameter estimation method.[52] A demonstration of the technique was made using both synthetic and experimental data. In addition to extracting kinetic and mechanistic information from chronoamperometric data, the problem of modeling responses produced by microelectrode arrays has also been addressed. Weisshaar and Tallman[53] reported an investigation of Kel-F-graphite composite electrodes using chronoamperometry and a model developed for partially blocked electrode surfaces. A simplex-based direct search was therefore employed to estimate the model parameters.

In each of the preceding applications simple nonlinear regression procedures were successfully employed to fit data from a variety of polarographic, voltammetric, and chronoamperometric experiments. Additionally, applications of nonlinear regression methods have also appeared in the analysis of impedance and admittance data.[54,55] Although all of the foregoing studies reported good results, relatively few of the authors adequately addressed the issue of errors in the parameter estimates obtained in the nonlinear fits. This is a critical weakness in any nonlinear regression study, because analytical expressions for error tolerances are not readily available. Further, the existence of correlation between the parameters being estimated in a nonlinear regression, a situation that is frequently encountered in electrochemical kinetics, complicates the correct assignment of the error tolerances. A contributing factor to this problem is the issue of selecting a proper set of weighting coefficients for the regression, another critical issue that has been given too little attention in the majority of nonlinear regression studies.

Up to this point only limited use of electrochemical simulations as models in nonlinear regression has been discussed. In the work of Hanafey et al.,[29] direct coupling of the simulations into the nonlinear regression

routines was limited due to the prohibitive computational burden. One solution was demonstrated by Arena and Rusling,[56] who made use of the more computationally efficient expanding space grid, explicit finite difference simulations. In addition to the efficient simulation model, the authors also employed a more efficient estimation and fitting method, a Levenberg-Marquardt algorithm. This combination made the simulation/regression procedure less computationally demanding. Even with the reduction in computational load, an entire simulation must be run at *each iteration* in the regression.

B. Recursive Methods for Nonlinear Regression

Kalman filtering has been used for parameter estimation in a number of examples in the electrochemical literature. As in the previously discussed methods, the models being fitted to the data are nonlinear. The nonlinear form of the model prevents the use of the simpler, linear, discrete Kalman filter discussed previously. Several modifications to the basic Kalman filter algorithm exist for use in nonlinear optimization problems, including the extended Kalman filter, the extended-iterated Kalman filter, second- (and higher) order Kalman filters, and the linearized Kalman filter. Of these, only the extended and the iterated-extended Kalman filters have been applied to electrochemical problems.

An extended Kalman filter can be designed to handle problems with nonlinear measurement models, nonlinear system dynamics, or both. The extended Kalman filter is based on expanding the nonlinear system dynamics and nonlinear measurement models in a Taylor series about the current trajectory of the state vector. The functions are then linearized by truncating the series after the linear terms, which defines the linearized system dynamics and measurement matrices. The remainder of the filter algorithm is identical to that of the linear, discrete Kalman filter. Details of the extended filter are given by Brown.[11]

Some of the most interesting applications of Kalman filtering in electrochemistry have exploited the recursive nature of the algorithm as an efficient means of optimizing a simulation while simultaneously fitting the simulation model to a set of data. Using an electrochemical simulation as the model in a nonlinear regression can be done in a number of different ways. In the optimization schemes discussed previously, it was necessary to run an entire simulation, which can require a significant amount of computer time, for each successive evaluation of the object function. If an optimization required 100 iterations to converge on a set of parameter estimates, a minimum of 100 separate simulations needed to be run in the process. Brown et al.[57] were the first to couple a simulation for linear sweep voltammetry to an extended Kalman filter to perform the optimization recursively. The authors used the method to estimate the standard rate constant and charge transfer coefficient for simple heterogeneous electron transfer reactions. In this approach, the filter is provided with a data set to be fitted and the initial guesses for the parameters to be estimated. As the simulation is being run, it is optimized recursively by evaluating the filter object function and adjustment of the parameter estimates used in the simulation as each successive point in the experimental voltammogram becomes available. Thus, it is possible to perform the nonlinear regression and obtain the desired parameter estimates by running only a single simulation. Because the computational overhead required by the Kalman filter is small (about 10%) compared to the computations involved in the simulation, a reduction in computing time of several orders of magnitude was realized.

Lavagnini et al.[58] have also reported the use of an extended Kalman filter to optimize a simulation for cyclic voltammetry. In this study the authors used the filter to estimate the $E^{O'}$ values for a reversible EE mechanism. In addition to the extended filter, an iterated extended filter, simplex, and Marquardt optimizations were also employed and the relative performances were compared. The authors reported that all three of the

methods yielded accurate estimates for the $E^{O\prime}$ values. As part of the study the computer times required for each of the estimations were also reported. From the values reported, it appears that the filter was not used to recursively optimize the simulations, but rather an entire simulation was run for each iteration of the filter. Although this approach is consistent with the manner in which a simulation is coupled to other optimization routines, it does not take advantage of the tremendous reduction in computational time achieved by performing the optimization recursively.

Recently Bear and Brown extended the work of Brown et al.[57] to fit voltammetric responses generated in potential-step experiments.[59] In this work, the EFD simulation was generalized, enabling the EFD technique to be used with any potential-step protocol. Four different types of potential-step experiments were examined using both synthetic and experimental data: staircase voltammetry, square-wave voltammetry, a large-amplitude version of staircase voltammetry, and pseudorandom potential-step voltammetry. Data for each of the different voltammetric techniques were fit using the same Kalman-filter-optimized simulation routine. A typical fit using synthetic data for pseudorandom potential-step voltammetry is shown in Figure 6. The kinetic parameters in the simulation were estimated with very good accuracy, and the estimates were independent of the specific voltammetric technique employed. Further, the authors reported that applied potential sequences with more random character produced kinetic parameter estimates with higher precision. A Monte Carlo technique was used to assess the precision of the parameter estimates obtained. The computational advantages of performing the fitting recursively were also illustrated. The explicit finite difference simulation of a staircase voltammogram required 76.2 s; fitting the same voltammogram using the Kalman-filter-optimized simulation required only 78.9 s. Only a small increase in computa-

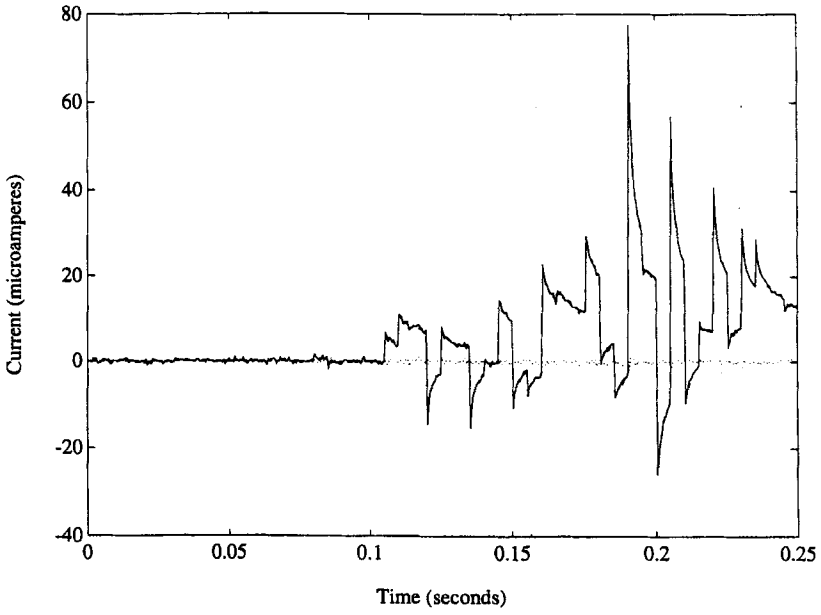

FIGURE 6. Kalman filter fit of a synthetic, pseudorandom pulse voltammogram for a system displaying quasireversible kinetic behavior. Random noise was added to the data to give a peak signal-to-noise ratio of 200. The synthetic voltammogram (solid line), the filter-generated fit (dashed line), and the filter innovations (dotted line) are all displayed.

tional time — relative to the time used to run a single simulation — is required by this recursive optimization procedure.

C. Parameter Estimation by Calibration to Data Features

An alternative method to voltammetric parameter estimation has been described by Speiser,[60] and further work on the method has also been reported.[61-63] Speiser's approach is based on developing empirical correlations between relevant system parameters, such as heterogeneous and homogeneous rate constants, and the characteristics of voltammetric responses produced by these systems. The author(s) developed a simulation package to generate voltammograms that model a wide range of system kinetics, producing "working curves", for each of the mechanisms under study. Key features, such as peak position, are extracted from the series of voltammograms. Regression analysis is then used to correlate those features extracted from the voltammetric response to the system's kinetic parameters. Both MLR and B-spline regression have been used by the author(s) for generating the empirical models. Once the empirical model has been established, it can be used for the analysis of sample voltammograms. Voltammetric features from the sample voltammogram are used in the model to predict the appropriate system parameters for the mechanism under study. The system parameters obtained in the prediction step are then used in the corresponding simulation to generate a synthetic voltammogram. This synthetic response is then compared with the experimental data. If the observed fit is good, the procedure is terminated and the parameter values are reported. An observed lack of fit indicates the need to repeat the procedure with another model. In principle this is very similar to the working-curve approach of Hanafey et al.[29] discussed before, yet it has several distinct advantages. By reducing the data from an entire voltammetric response to a set of descriptive parameters and by using a simple empirical correlation, the computational and storage requirements are dramatically reduced. The resulting simulation and analysis routines make up a much smaller, yet easy to use, software package.

D. Global Methods of Parameter Estimation

Global analysis of voltammetric data[64-66] has been proposed recently for the estimation of heterogeneous kinetic parameters from systems displaying an E mechanism. Although this approach does not employ any sophisticated chemometric techniques, it is a novel way of transforming and analyzing voltammetric data, and it may deserve further study. The principle behind this method is that the kinetic parameters for the electrode reaction will be uniquely described in a three-dimensional space, which is defined by the applied potential, the current, and the semiintegral of the current. The resulting analysis is reduced to a simple graphical representation. Once this reduction is accomplished, a weighted linear regression is applied to obtain the parameter estimates.

IV. OPTIMIZATION

The extraction of relevant information from chemical data is important, but it is equally important to employ sound experimental design in acquiring the data. Chemometrics is also concerned with the design of experiments that produce maximum information in the data, while making the measurement process more efficient. In the foregoing discussion, optimization methods were employed to drive nonlinear regressions for fitting experimental data. However, optimization methods are not limited to use in regression procedures. Optimization methods can be readily applied to the problem of experimental design.

Relatively few applications of experimental design have been reported in the electrochemical literature. Copeland et al.[67] reported one of the first applications of experimental design in electroanalytical chem-

istry. In this work, the authors applied a factorial design to optimize and assess the performance characteristics of differential-pulse, anodic-stripping voltammetry at thin film mercury electrodes. With the factorial design the authors characterized the effects of both instrumental and experimental parameters to obtain a set of optimum conditions for the determination of trace levels of Pb(II) and Cd(II) in water, urine, and blood specimens.

Although other examples of optimizing experimental conditions have appeared, such as a study of computer-assisted, interactive optimization of anodic-stripping voltammetry given by Thomas et al.,[68] very few have employed a statistically sound experimental design protocol. A recent exception was presented by Oduoza,[69] who addressed the issue of simplex optimization of electroanalytical experiments. In this work the author illustrated the use of computerized control and optimization of a staircase voltammetry experiment. The analysis provided a compromise between sensitivity and resolution in the voltammetric data. Only two parameters were used in this optimization, the potential-step height and step duration, but extension of the principles used here would be straightforward. Other authors have considered the problem of optimizing the performance of electrochemical detectors for flow-injection experiments.[70] The results were examined graphically, where the optimum conditions were represented by a bounded region of performance parameters. Glass et al.[71] have applied the Shannon entropy as a criterion in optimizing the information content provided by multielement, microelectrode arrays. The authors examined the information gain produced by using a microelectrode array composed of five elements (Pt, Au, V, Ir, and C) over that from a single Pt microelectrode. They also applied information-based optimization to studies of materials by cyclic voltammetry with the microelectrode array. Two sets of compounds were analyzed; one set was composed of high explosives and the other was a set of structurally similar compounds. The authors reported a 25% gain in the information content when the multielement microelectrode array was used.

The application of experimental design is widespread throughout the remainder of analytical chemistry, far surpassing the rate at which applications appear in the electroanalytical literature. At first this fact would seem a bit disturbing, but on further consideration one might propose the following explanation. The majority of articles on electrochemistry encountered in preparing this review dealt primarily with the theoretical aspects of methods and reaction mechanisms. Most applications of experimental design observed in other fields of chemistry were oriented toward the optimization of conditions and operating parameters associated with the implementation of methods for routine analysis. These two different orientations should not be considered to be mutually exclusive. The application of statistically sound experimental design methods can only improve the results obtained in any analysis.

V. SIGNAL PROCESSING

Signal processing is a discipline of chemometrics that is concerned with the manipulation of analytical data to make the information contained in the data more accessible. These manipulations can take many forms, ranging from smoothing a data set for suppressing experimental noise to deconvoluting data for enhancing resolution. Simple signal processing techniques are among the most commonly practiced chemometric methods in electroanalytical chemistry. Many applications of signal processing principles in electrochemistry are concerned with electrochemical theory, such as convolution voltammetry, and will not be considered here. Applications of signal processing that are focused on instrumentation or experimental techniques, such as Fourier Faradaic admittance measurements, are also omitted from this review. Methods that are discussed are those whose applications are not unique to electroanalytical chemistry, but have been applied here for enhancement of the data analysis. A good introduction to signal processing in electrochemistry was given by Smith.[72,73] This article was presented in two

parts and covered an introduction to Fourier transform Faradaic admittance measurements as well as discussions of the data enhancement methods.

A. Methods Using the Fourier Transform

A majority of the signal processing methods applied in electrochemistry are based on the use of the Fourier transform and its properties.[74] In addition to providing frequency domain information for analyses, where this is the primary concern, the Fourier transform also provides a convenient numerical means of performing other types of data enhancements. Because most modern instrumentation records data as discretely sampled events, a discrete formulation of the Fourier transform pair is used in actual computations. The discrete, band-limited, Fourier transform pair is

$$H_n = \sum_{n=0}^{N-1} h_k \, e^{2\pi jkn/N} \qquad (27)$$

$$h_k = \frac{1}{N} \sum_{n=0}^{N-1} H_n \, e^{-2\pi jkn/N} \qquad (28)$$

where H_n is the nth frequency component, h_k is the kth time sample, N is the number of samples in the data set, and $j = \sqrt{-1}$. In this representation, the factor of 2π is always given in the exponential, a convenience that can eliminate some confusion in the notation.

1. Fourier Smoothing

One of the most frequently exploited features of the time and frequency domain representations of data is the relative locations of signal and noise components in each case. In most analytical data the signal components are characterized by large-amplitude, slowly varying responses, whereas the noise is usually observed as rapidly changing, small-amplitude fluctuations. For most systems this description, which assumes that the noise is random or "white" in character, is valid. In the frequency domain the situation is quite different: information describing the signal components is contained in the low-frequency region of the spectrum, whereas the white noise distributes across the entire spectral range.

The entire Fourier transform contains both real and imaginary frequency components. Because experimental data consist only of real numbers, the imaginary portion of the spectrum contains a mirror image of the real spectrum. Although the redundant information contained in the imaginary component is not used in most applications, it should be included in the calculations to prevent violating Parseval's theorem.[4,74] If only the real frequency components are used in subsequent calculations, the results must be adjusted by a factor of 2 to retain the same total integrated power. Many authors using transform methods seem to forget this fact.

By determining the frequency beyond which little or no signal information is present, it is possible to effectively remove most of the noise from the data. The Fourier transform is multiplied by a step function, or other suitable apodizing function, to set the high-frequency coefficients to zero while leaving those corresponding to the signal components unaltered. After this multiplication has been carried out, the resulting spectrum is inverse-transformed to the original data domain. A substantial reduction in the noise level is obtained by this Fourier filtering procedure. This process is illustrated in Figure 7, which depicts the Fourier filtering of a noisy square-wave voltammogram.

Examples of Fourier smoothing have been appearing in the electrochemical literature since the early 1970s.[75] Recently, a new algorithm for Fourier smoothing of electrochemical data was reported by Aubanel et al.[76] This algorithm uses an alternative to the commonly employed fast Fourier transform (FFT) that takes advantage of the fact that experimental data consist of real numbers, eliminating the need for the complex portion of the transform. This consideration reduces both the computational and storage requirements for the transform. Although the authors have proposed their own algorithm,

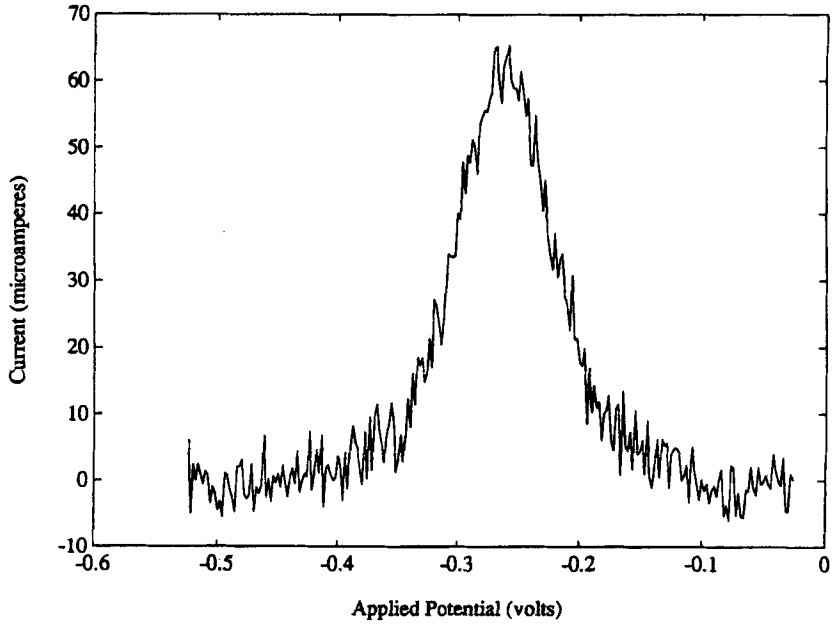

(a)

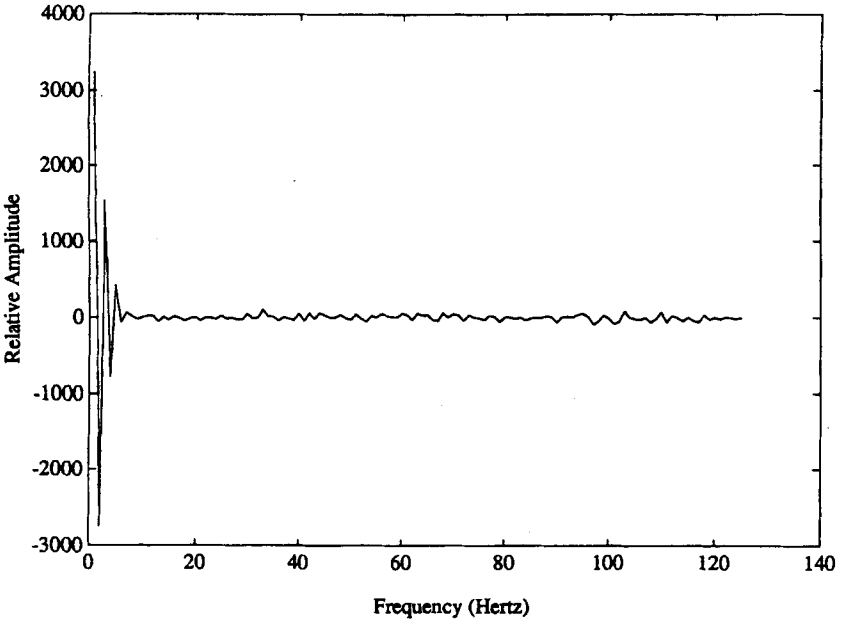

(b)

FIGURE 7. (a) Noisy square-wave voltammogram, (b) Fourier transform of the noisy square-wave voltammogram.

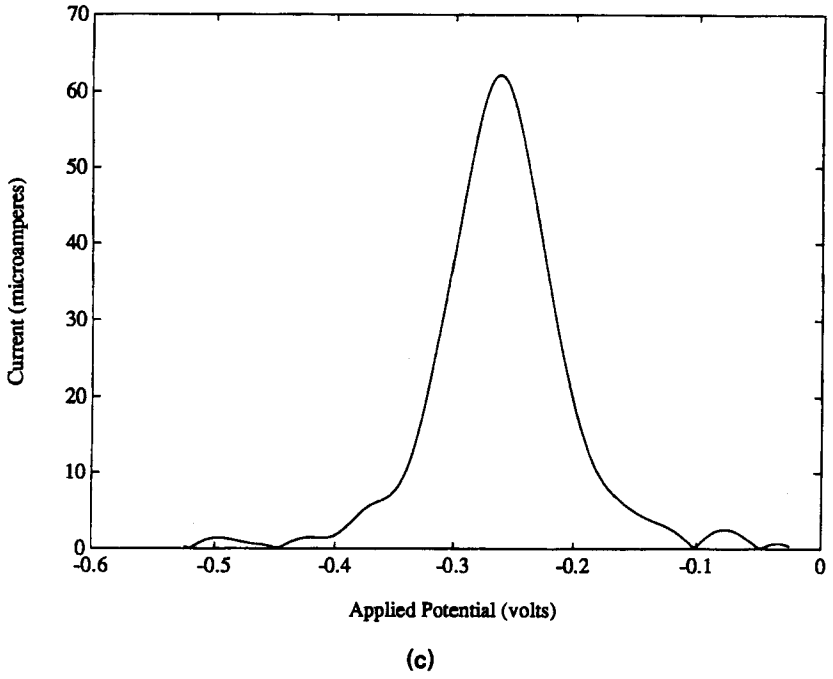

FIGURE 7. (c) Fourier filtered, square-wave voltammogram.

similar results can be obtained through efficient use of either the standard FFT or the Hartley transform, a real version of the FFT.[4] In addition to their transform algorithm the authors proposed an alternative to the standard step function frequently used in Fourier smoothing; the new function helps to reduce the ringing commonly associated with using the step function.

2. Fourier Interpolation

Other authors have applied the Fourier transform to the interpolation of sparse electrochemical data.[77] The interpolation was proposed to better define the peak location in such data sets. Interpolation of a data set is performed by transforming the original data set to the Fourier domain, padding the transformed data with zeros, then applying the inverse transform to return to the original data domain. As an example, consider a data set containing only sparse data points that has been transformed to the Fourier domain. By the addition of zeros (padding) to the end of the transformed data and inverse transforming, the number of points in the data set is increased. The number of points in the new data set will be equal to the sum of the original data and the number of zeros added. At a first glance this procedure may appear to work wonders, but no information has been added to the original data despite the increase in the number of data points.

3. Parameter Estimation in the Fourier Domain

Performing parameter estimation in the Fourier domain was reported by Binkley and Dessy,[78] who used linear LSR in the Fourier domain to resolve overlapped square wave voltammograms. This application takes advantage of the linear nature of the Fourier transform, which can be stated as the following: the Fourier transform of a summed response is equal to the sum of the transforms of the individual responses. Because the responses are additive in both domains, parameter estimation can readily be performed in either. An advantage gained by this approach is a reduction in the dimensionality of the problem. The signal information is contained

in the low-frequency portion of the spectrum, which allows the size of the data set to be reduced from the original number of data points in the sampled voltammogram to the first few frequency coefficients that contain relevant signal information. This reduction in the dimensions of the data matrix results in a better conditioned problem for use with MLR.

4. Fourier Deconvolution

Another advantageous property of the Fourier transform that has been addressed in electrochemistry is the ease in dealing with convolution problems. The convolution theorem is stated as, "the Fourier transform of two functions convoluted in the time/potential domain is equal to the product of the Fourier transforms of the individual functions," where the discrete convolution of two functions, h and g, is defined as

$$(h^*g)_k = \sum_{-\tau=M/2}^{M/2} g_{k-\tau}h_\tau \qquad (29)$$

and M is the duration of the response function h.

The convolution properties of the Fourier transform allow for resolution enhancement by the deconvolution of responses with an appropriate function. Deconvolution is performed by dividing the Fourier transform of the convoluted response by the transform of the appropriate convoluting function, and then performing an inverse transform on the results. The new data set obtained from this procedure has the artifacts of the convoluting function removed. Many examples of this approach have been reported in electrochemistry. These have ranged from sharpening AC polarographic peaks by deconvoluting with a function based on the expected system response[79] to similar methods applied to the study of adsorption effects using differential pulse polarography.[80]

Theoretical studies of the Fourier transform of voltammetric peaks, waves, and reversible linear sweep voltammograms have also been undertaken.[81-84] With the results obtained in the latter theoretical studies, the authors were able to apply deconvolution for resolving overlapping voltammetric responses. This type of procedure has also been applied to the removal of instrumental artifacts from voltammetric measurements.[85] Deconvolution was used to remove the effects of slow current transducers observed in voltammetric studies with ultramicroelectrodes and high potential sweep rates.

5. Fourier Differentiation

Numerical differentiation of data is another application of the Fourier transform. Differentiation and integration of data are based on the following property of the transform:

$$\frac{d^m h_k}{dk^m} = \frac{1}{N}\sum_{n=0}^{N-1}(2\pi jn)^m H_n e^{-2\pi jkn/N} \qquad (30)$$

where m is the order of differentiation, or integration if the sign of m is negative. Multiplying the Fourier transform of a data set by $(2\pi if)^m$, then performing the inverse transform results in the numerically differentiated data. For example, to obtain the first derivative of a data set, the Fourier transform of the data set would be multiplied by a linear ramp. The resulting frequency domain function is then inverse-transformed to yield the derivative of the original data. de Levie et al.[86] have applied this technique to interfacial tension data. In this procedure the data set was simultaneously smoothed and differentiated.

B. Kalman Filtering

Smoothing of electrochemical data can be performed in a number of ways. The preceding discussion focused on the application of Fourier smoothing, but other methods such as Savitzky-Golay filtering/smoothing and the Kalman filter also can be used. Lavagnini et al.[87] reported on the use of the

Kalman filter for smoothing, calibration, and solution equilibria problems. In this work the authors compared the performance of Kalman, Savitzky-Golay, and Fourier filtering for smoothing voltammetric data. Although the Kalman filter can be implemented as a true, real-time filtering method, the authors report some minor problems with asymmetry in such cases. To avoid distortion of data by filter asymmetry, the Kalman filter can be used as an optimal smoother after data collection, allowing both forward and backward passes through the data to be made.

VI. PATTERN RECOGNITION

Pattern recognition is the common name for a widely applied discipline of chemometrics that is concerned with classification and identification of samples. Its applications are routine in the general literature of analytical chemistry, but much of the work reported in the electrochemical literature was done in the early days of chemometrics and is therefore based on older methods. The studies that have appeared have focused on the use of three simple pattern recognition methods: linear learning machines, *k*-nearest neighbors classification, and expert systems. Other, more sophisticated pattern recognition methods are routinely applied in other fields of analytical chemistry. The interested reader is referred to standard chemometric texts[3,19] for details on these.

The purpose of pattern recognition is to develop a semiquantitative model that can be applied to the identification of unknown sample patterns. Each sample "pattern" or "object" contains N response variables, which may or may not be mean-centered, scaled, or otherwise transformed to enhance the data analysis to follow. Transformed variables, even those that are not changed at all, are generally called "features". With N features, each object in the data is described by a vector in a space of N dimensions. Each of the different pattern recognition methods seeks to describe how the samples of known class are oriented with respect to each other and those of other classes in the multidimensional space. By establishing similarities between data for samples of known class and then exploiting these similarities, unknown samples can be classified. Unlike other areas of chemometrics, however, the classification of multivariate data is best done with the aid of several methods, so that the clearest picture of the data and class structures can be obtained. For this reason, the brief overviews of the relevant methods used in pattern classification will be given first, and the applications of pattern recognition will follow this discussion.

A. Linear Learning Machine

The linear learning machine is a simple, binary classification technique that can be applied to problems where the mulivariate data are linearly separable. This technique was one of the first pattern recognition methods applied in the field of chemistry, mainly due to its simplicity and ease of programming. It is an iterative method, and, as with any iterative method, finding a solution can be time-consuming, especially when an ill-selected starting point is used. For classifying a linearly separable problem with sufficient data, the linear learning machine classifier works well, but other methods, such as statistical linear discriminant analysis,[3,19] offer a more efficient approach for linearly separable problems. Although the basic algorithm for linear learning machines was designed to define a decision threshold between two classes, sequential applications of the algorithm can extend its utility to a larger number of classes, at the cost of time.[19]

The requirement that the problem is linearly separable will become apparent through an example of how the linear learning machine performs a classification. Consider a data set containing patterns, which are represented by the coordinates on two feature axes, for two classes (A and B). In the data, two distinct groupings, or clusters, are observed that correspond to the two classifications. If the data space is augmented by one dimension, with each pattern assigned a value of unity along that axis, it becomes possible

to separate the data clusters using a plane in the $N + 1$ dimensional space. In the augmented data space this plane is uniquely defined by a normal weight vector (**w**) that passes through the origin. Initially, the linear learning machine positions the plane at random. By determining the dot product of the weight and object vectors, the position of any object is either positive or negative with respect to the plane (i.e., a simple binary classification results, depending on which side of the plane the object falls). In refining the position of the plane the algorithm calculates if any of the B samples have been classified on the A side of the hyperplane. When the first B sample is encountered on the A side, the linear learning machine calculates a new estimate for the position of the hyperplane. This trial and error process is repeated until all of the A samples reside on one side of the hyperplane and all of the B samples are on the other. After the linear learning machine has "learned" the training set, test samples can be classified by calculating on which side of the decision plane they fall.

B. *k*-Nearest Neighbors Classifier

k-nearest neighbors classification is the second oldest pattern recognition technique with applications reported in the electrochemical literature.[19] This technique is also simple, easily programmed, and, despite its simplicity, can yield very accurate classifications for a wide range of problems. The classification is based solely on the relative proximity, or distance in the multidimensional feature space, of the test pattern to neighboring samples of known class. Distances between the sample pattern and all patterns in the training set are calculated. These distances are then examined in ascending order. The class sample with the shortest distance to the test sample — the nearest neighbor — provides the closest match to the characteristics of the test sample and is the first approximation for determining the class of the unknown. Each of the first k neighbors, where k is a number selected by the user, is used to provide a "vote" in the unknown's classification. If the unknown sample is located near the center of the training patterns for one class and there are no members of other classes nearby, all k votes will be of the same class. This will remain true until the number of neighbors being examined exceeds the number of members in the class. In cases where the test sample lies in a region between samples of different classes or if the classes are diffuse, then the *k*-nearest neighbors will contain a mixture of different class "votes".

There are several key requirements for accurate classifications using the *k*-nearest neighbors method. First, the data need to have well-resolved clusters present for each class. Second, an adequate number of samples must be present to define each of the known classes, relative to the number of neighbors used to evaluate the class of the unknown. Additionally, each of the training set samples must be correctly classified. In problems where there are insufficient samples, large discrepancies in the number of training samples that represent each class, or overlapped clusters, *k*-nearest neighbors classification will be limited in its ability to accurately assign classes to unknown samples.

C. Expert Systems

The third method that has been used for classification in electrochemistry is the expert system, which is a simple hierarchy of user-defined rules that are used to evaluate the data. An expert system translates a heuristic method into a decision tree that can be implemented to automate the analysis of data for a particular problem. Although this method is conceptually simple and easy to implement, it suffers from some severe drawbacks. The classification accuracy is based solely on the programmers' understanding of the problem and their ability to foresee the flow of difficult-to-classify samples through the decision tree. One possible advantage of the expert system is that it may not require a traditional training set to establish the

classification rules. Because the expert system rules must be established by some means, some sort of training data is needed.

D. Pattern Recognition Applied to Resolution

Applications of the linear learning machine in electrochemistry represent some of the first reported uses of chemometric methods in the field. Sybrandt and Perone[88,89] were among the first to apply this technique for the qualitative analysis of mixtures in stationary electrode polarography. In these studies, the authors suggested that the resolution of the classification method was primarily limited by the precision of experimental data. Derivatization was also investigated as a pretreatment for the polarographic data. Early studies by Ichise et al.,[90] which utilized an analog-feedback linear learning machine, were focused on the identification and quantitation of analytes in mixtures. The authors reported a quantitation error of 10% for the analytes in a four-component mixture.

The identification of overlapping voltammetric responses from single voltammograms has been addressed using both *k*-nearest neighbors and linear learning machine classifiers by Thomas and co-workers.[91,92] One of the key aspects addressed in these studies was the selection of features to be used in the pattern recognition. By Fourier transforming the experimental voltammograms and truncating the transformed data after the first few Fourier coefficients, Thomas et al. effectively reduced the dimensionality of the problem. With the reduced number of features the doublet/singlet peak classification was made more efficient and effective. In studies using both experimental and synthetic voltammograms the procedures developed were reported to reliably identify the multiplets. The authors recommended the use of *k*-nearest neighbors classifier over the linear learning machine; this version of the method was later implemented in an on-line configuration.[93] Figure 8 illustrates a training set composed of well-characterized, experimental data, showing two of the three features used in the classification. As with the other methods discussed earlier for resolving/identifying overlapped responses, the performance of the *k*-nearest neighbors classification was a function of the relative peak heights for the individual components. Reliable classifications were only obtained for peak height ratios of less than 5:1, with some degradation of performance observed outside of this range.

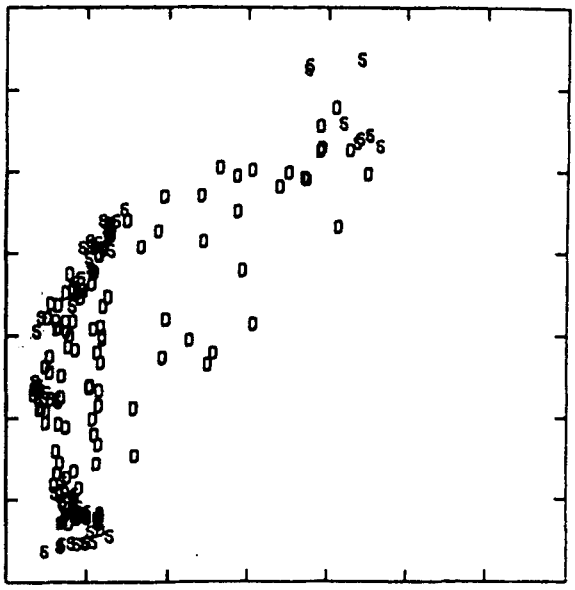

FIGURE 8. Feature plot of real singlets and real doublets from the PRED1[85] data set. S = singlet; D = doublet. (Reprinted from DePalma, R. A.; Perone, S. P. *Anal. Chem.* **1979**, *51*, 825–828. With permission. Copyright 1979, The American Chemical Society.)

E. Pattern Recognition in Kinetic Studies

k-nearest neighbors classification of Fourier-transformed voltammograms was also used by DePalma and Perone[94] for the evaluation of electrochemical kinetic parameters of simple heterogeneous electron transfer reactions. This procedure was based on matching the shape of the transformed voltammograms to that of numerically generated voltammograms with known kinetic parameters. A training set composed of 2310 synthetic voltammograms was used to provide the known kinetic responses. Prior to applying the Fourier transform, each of the

voltammograms was normalized to unit height and translocated along the potential (time) axis, such that the current maximum occurred at the 96th point of the 128 data points used for the transform. The authors evaluated the kinetic parameters of a sample voltammogram as the average of those corresponding to the four nearest neighbors in the training set that used the first 15 Fourier coefficients to define the feature space. Accurate parameter estimates were obtained in studies using both synthetic data and experimental data. To prevent the improper classification of nonrepresentative test samples, the distances to each of the neighbors was required to be less than a critical value. Attempts to classify samples that were not represented in the training set, such as that from two overlapped responses, resulted in the critical distance being exceeded. The consideration of the critical distance in the classification is a good feature that identifies outliers present in the test data.

F. Identification of Electrochemical Mechanisms

A series of papers by Ichise et al.[95-99] reported applications of simple pattern recognition methods for the extraction of qualitative information about the electrode process in a voltammetric experiment. As a method of compressing the data to generate a better defined feature space, the authors explored the use of Hadamard and Walsh transforms. Other authors also explored the use of pattern recognition for the identification of electrochemical mechanisms. Schachterle and Perone[100] extended the methods previously developed with *k*-nearest neighbors classification using Fourier-transformed voltammograms to accommodate the classification of electrochemical mechanisms. As in the previous work from Perone's laboratory, the authors used synthetic data, generated for a series of mechanisms under a range of experimental conditions, to form the training set for the pattern recognition. In this study, both cyclic voltammetry and cyclic staircase voltammetry were employed to collect the experimental data. In addition to the Fourier-transformed voltammograms, the authors also used the anodic and cathodic peak separation and peak current ratios as additional features for each object studied. For studies that combined the two sets of data for pattern recognition features, the authors used autoscaling to prevent unintentional weighting of specific feature variables. Extensions of the foregoing method were reported for applications in the characterization of the structure-activity relations of selected organic compounds.[101,102] For this classification, staircase voltammograms and differential capacity curves were used as the basis for the *k*-nearest neighbors classifications. Although good results were reported for the range of samples used in these studies, little has been reported in the way of extensions or applications.

Other methods have also been presented for the automated classification of electrochemical mechanisms based on voltammetric data. Rusling[103,104] implemented a technique termed deviation-pattern recognition, a classification performed on the residuals produced by nonlinear regression fits to an experimental voltammogram. The basic method employed is an expert system that guides the process of performing a nonlinear regression, analyzing the deviation scatter plot, and selecting the next appropriate trial mechanism. Initially, all input data sets are fitted with a nonlinear regression to the same mechanism; the analysis of the residuals then determines the path taken through the decision tree. The classification automatically proceeds until the correct mechanism is identified, as indicated by a random distribution of regression residuals, or until the expert system is unable to match the voltammogram with any of the mechanisms present in the identification tree. Because the foregoing scheme performs a regression to fit the voltammogram for each of the mechanisms being tested, estimates of the relative electrochemical parameters are also obtained. A simplified version of this scheme was used by Rusling and Connors[105] to distinguish overlapped, catalytic voltammograms from those corresponding to noncatalytic systems.

Palys et al.[106] have also implemented an expert system for the elucidation of electrode mechanisms. In this paper the authors reported an automated method for analyzing data from sampled DC polarography to determine the appropriate mechanism. In the expert system, a set of diagnostic criteria for the different electrode mechanisms under study are evaluated. Based on the results obtained, the mechanism is identified by its position in the decision tree. The main advancement presented in this work is the direct coupling of both the data analysis and the experimental control to the expert system. In this dual role, the system is almost completely automated. A more advanced version of this system has also been reported by the same authors.[107] Staircase voltammetry, convolution voltammetry, and chronocoulometry are all part of the expert system's experimental repertoire in this latest report. The expert system designs experiments, controls the voltammetric or coulometric run, and collects data for each of the experiments used in the automated mechanism elucidation. The authors state that a complete cycle using the improved system requires about 25 min to determine an electrode mechanism, as compared to the 8 h reported in the earlier work.

VII. CONCLUSIONS

The current availability of high-performance, low-cost computers has removed one of the most significant barriers to the routine application of sophisticated data analysis methods. The other major barrier, the lack of familiarity with these methods, is only slowly yielding to progress in the field.

In this review a wide range of applications for chemometrics in electrochemistry have been presented. Although the articles selected represent only a sampling of these applications, distinct trends in the field are apparent. First, the portion of papers in electroanalytical chemistry reporting the use of chemometrics appears to be lower than that observed in analytical chemistry as a whole. Second, despite this lower proportion of papers, chemometric methods have made regular appearances in the electrochemical literature over the past 2 decades.

Much progress has been made in applying chemometrics to electrochemical problems, but there remains a tremendous potential for advancement. The application of multivariate calibration in electrochemistry is one area where we expect to see substantial growth in the future. Those studies that reported the use of multivariate methods, such as MLR and PLS regression, are a sign that modern chemometric techniques are beginning to permeate all areas of electroanalytical chemistry. We hope that our emphasis on the few appearances of factor-based techniques illustrates the power and potential applications of these methods. The second area we hope to see expand is pattern recognition in electrochemistry, which has been almost dormant during the recent past. In other areas of analytical chemistry, pattern recognition has become a routine tool with applications being reported on a regular basis. Both of these areas, in addition to all applications of chemometrics in electrochemistry, should continue to grow as researchers become more aware of successful applications of chemometrics in electroanalytical chemistry.

REFERENCES

1. Otto, M. *Anal. Proc.* **1987**, *24*, 335–336.
2. Otto, M.; Thomas, J.D.R. *Ion-Selective Electrode Rev.* **1986**, *8*, 55–84.
3. Massart, D.L.; Vandeginste, B.G.M.; Deming, S. N.; Michotte, Y.; Kaufman, L. *Chemometrics: A Textbook*; Elsevier: Amsterdam, 1988.
4. Press, W. H.; Flannery, B.P.; Teukolsky, S.A.; Vetterling, W.T. *Numerical Recipes: The Art of Scientific Computing;* Cambridge University Press: Cambridge, 1986.
5. Turnes, G.; Cladera, A.; Gomez, E.; Estela, J.M.; Cerda, V. *J. Electroanal. Chem.* **1992**, *338*, 49–60.
6. Beebe, K.; Uerz, D.; Sandifer, J.; Kowalski, B. *Anal. Chem.* **1988**, *60*, 66–71.
7. Otto, M.; Thomas, J.D.R. *Anal. Chem.* **1985**, *57*, 2647–2651.
8. Liteanu, C.; Hopirtean, E.; Popescu, I.C. *Anal. Chem.* **1976**, *48*, 2013–2019.
9. Liteanu, C.; Hopirtean, E.; Popescu, I.C.; Rica, I.; Stefaniga, E. *Anal. Chem.* **1978**, *50*, 1202–1209.

10. Jain, R.; Schultz, J.S. *Anal. Chem.* **1984**, *56*, 141–147.
11. Brown, S.D. *Anal. Chim. Acta* **1986**, *181*, 1–26.
12. Seelig, P.F.; Blount, H.N. *Anal. Chem.* **1976**, *48*, 252–258.
13. Seelig, P.F.; Blount, H.N. *Anal. Chem.* **1979**, *51*, 327–337.
14. Seelig, P.F.; Blount, H.N. *Anal. Chem.* **1979**, *51*, 1129–1134.
15. Brown, T.F.; Brown, S.D. *Anal. Chem.* **1981**, *53*, 1410–1417.
16. Scolari, C.A.; Brown, S.D. *Anal. Chim. Acta* **1984**, *166*, 253–260.
17. Malinowski, E.R. *Factor Analysis in Chemistry*, 2nd ed.; Wiley-Interscience: New York, 1991.
18. Martens, H.; Næs, T. *Multivariate Calibration*; Wiley: Chichester, 1989.
19. Sharaf, M.A.; Illman, D.L.; Kowalski, B.R. *Chemometrics*; Wiley-Interscience: New York, 1986.
20. Howery, D.G. *Bull. Chem. Soc. Jpn.* **1972**, *45*, 2643–2644.
21. Keller, H.R.; Massart, D.L. *Chemom. Intell. Lab. Syst.* **1992**, *12*, 209–224.
22. Kankare, J.; Lukkari, J.; Pajunen, T.; Ahonen, J. *J. Electroanal. Chem.* **1990**, *249*, 59–72.
23. Henrion, A.; Henrion, R.; Henrion, G.; Scholz, F. *Electroanalysis* **1990**, *2*, 309–312.
24. Beebe, K.R.; Kowalski, B.R. *Anal. Chem.* **1988**, *60*, 2273–2278.
25. Hert, J.; Krogh, A.; Palmer, R.G. *Introduction to the Theory of Neural Computation*; Addison-Wesley: Redwood City, CA, 1991.
26. Bos, M.; Bos, A.; Van der Linden, W.E. *Anal. Chim. Acta* **1990**, *233*, 31–39.
27. Van der Linden, W.E.; Bos, M.; Bos, A. *Anal. Proc.* **1989**, *26*, 329–331.
28. Rusling, J.F. *Crit. Rev. Anal. Chem.* **1989**, *21*, 49–81.
29. Hanafey, M.K.; Scott, R.L.; Ridgway, T.H.; Reilley, C.N. *Anal. Chem.* **1978**, *50*, 116–137.
30. Bancroft, E.E.; Blount, H.N.; Hawkridge, F.M. *Anal. Chem.* **1986**, *58*, 2944–2949.
31. O'Dea, J.J.; Osteryoung, J.; Osteryoung, R.A. *J. Phys. Chem.* **1983**, *87*, 3911–3918.
32. O' Dea, J.; Osteryoung, J.; Lane, T. *J. Phys. Chem.* **1986**, *90*, 2761–2764.
33. O'Dea, J.J.; Wilkiel, K.; Osteryoung, J. *J. Phys. Chem.* **1990**, *94*, 3628–3636.
34. Osteryoung, J. *Chemom. Int. Lab. Syst.* **1991**, *10*, 141–154.
35. Go, W.S.; O'Dea, J.J.; Osteryoung, J. *J. Electroanal. Chem.* **1988**, *255*, 21–44.
36. Meites, L.; Lampugnani, L. *Anal. Chem.* **1973**, *45*, 1317–1324.
37. Bottecchia, O.L.; Degreve, L.; Boodts, F.C. *J. Electroanal. Chem.* **1990**, *285*, 37–47.
38. Boodts, J.F.C.; Bottecchia, O.L.; Degreve, L. *J. Electroanal. Chem.* **1987**, *223*, 79–89.
39. Colina, A.; Lopez Palacios, J.; Sarabia, L.A. *Chemom. Int. Lab. Syst.* **1989**, *6*, 81–87.
40. Birke, R.L.; Kim, M.H.; Strassfeld, M. *Anal. Chem.* **1981**, *53*, 852–856.
41. Kim, M.H. *Anal. Chem.* **1987**, *59*, 2136–2144.
42. Boudreau, P.A.; Perone, S.P. *Anal. Chem.* **1979**, *51*, 811–817.
43. Toman, J.J.; Brown, S.D. *Anal. Chem.* **1981**, *53*, 1497–1504.
44. Caster, D.M.; Toman, J.J.; Brown, S.D. *Anal. Chem.* **1983**, *55*, 2143–2147.
45. Rusling, J.F.; Connors, T.F. *Anal. Chem.* **1983**, *55*, 776–781.
46. Rodriguez Mellado, J.M. *J. Electroanal. Chem.* **1986**, *209*, 57–67.
47. Barbero, C.; Zon, M.A.; Fernandez, H. *J. Electroanal. Chem.* **1989**, *265*, 23–37.
48. Wanzhi, W.; Qingji, X.; Shouzhuo, Y. *J. Electroanal. Chem.* **1992**, *334*, 1–11.
49. Bergel, A.; Comtat, M. *J. Electroanal. Chem.* **1990**, *285*, 11–23.
50. Cheng, H.Y.; McCreery, R.L. *Anal. Chem.* **1978**, *50*, 645–648.
51. Rusling, J.F.; Brooks, M.Y.; Scheer, B.J.; Chou, T.T.; Shulkla, S.S.; Rossi, M. *Anal. Chem.* **1986**, *58*, 1942–1947.
52. Papanastasiou, G.; Kokkinidis, G.; Papadopoulos, N. *J. Electroanal. Chem.* **1991**, *305*, 19–36.
53. Weisshaar, D.E.; Tallman, D.E. *Anal. Chem.* **1983**, *55*, 1146–1151.
54. MacDonald, J.R.; Schoonman, J.; Lehnen, A.P. *J. Electroanal. Chem.* **1982**, *131*, 77–95.
55. Milocco, R.H. *J. Electroanal. Chem.* **1989**, *273*, 243–255.
56. Arena, J.V.; Rusling, J.F. *Anal. Chem.* **1986**, *58*, 1481–1488.
57. Brown, T.F.; Caster, D.M.; Brown, S.D. *Anal. Chem.* **1984**, *56*, 1214–1221.
58. Lavagnini, I.; Pastore, P.; Magno, F. *Anal. Chim. Acta* **1989**, *223*, 193–204.
59. Bear, R.S. Jr.; Brown, S.D. *Anal. Chem.* **1993**, *65*, 1061–1068.
60. Speiser, B. *Anal. Chem.* **1985**, *57*, 1390–1397.
61. Scharbert, B.; Speiser, B. *J. Chemom.* **1988**, *3*, 61–81.
62. Speiser, B. *Computers Chem.* **1990**, *14*, 127–140.
63. Speiser, B. *J. Electroanal. Chem.* **1991**, *301*, 15–35.
64. Bond, A.M.; Henderson, T.L.E.; Oldham, K.B. *J. Electroanal. Chem.* **1985**, *191*, 75–90.
65. Anderson, M.R.; Evans, D.H. *J. Electroanal. Chem.* **1987**, *230*, 273–280.
66. Zoski, C.G.; Oldham, K.B.; Mahon, P.J.; Henderson, T.L.E.; Bond, A.M. *J. Electroanal. Chem.* **1991**, *297*, 1–17.
67. Copeland, T.R.; Christie, J.H.; Osteryoung, R.A.; Skogerboe, R.K. *Anal. Chem.* **1973**, *45*, 2171–2174.
68. Thomas, Q.V.; Kryger, L.; Perone, S.P. *Anal. Chem.* **1976**, *48*, 761–766.

69. Oduoza, C.F. *Chemom. Intell. Lab. Syst.* **1992**, *17*, 243–248.
70. Elbicki, J.M.; Morgan, D.M.; Weber, S.G. *Anal. Chem.* **1984**, *56*, 978–985.
71. Glass, R.S.; Perone, S.P.; Ciarlo, D.R. *Anal. Chem.* **1990**, *62*, 1914–1918.
72. Smith, D.E. *Anal. Chem.* **1976**, *48*, 221A–240A.
73. Smith, D.E. *Anal. Chem.* **1976**, *48*, 517A–526A.
74. Bracewell, R.N., *The Fourier Transform and Its Applications*; McGraw-Hill: New York, 1965.
75. Hayes, J.W.; Glover, D.E.; Smith, D.E.; Overton, M.W. *Anal. Chem.* **1973**, *45*, 277–284.
76. Aubanel, E.E.; Myland, J.C.; Oldham, K.B.; Zoski, C.G. *J. Electroanal. Chem.* **1985**, *184*, 239–255.
77. O'Halloran, R.J.; Smith, D.E. *Anal. Chem.* **1978**, *50*, 1391–1394.
78. Binkley, D.P.; Dessy, R.E. *Anal. Chem.* **1980**, *52*, 1335–1344.
79. Grabaric, B.S.; O'Halloran, R.J.; Smith, D.E. *Anal. Chim. Acta* **1981**, *133*, 349–358.
80. Pizeta, I.; Lovric, M.; Zelic, M.; Branica, M. *J. Electroanal. Chem.* **1991**, *318*, 25–38.
81. Myland, J.C.; Oldham, K.B.; Zhu, G. *Anal. Chem.* **1988**, *60*, 1610–1621.
82. Engblom, S.O. *J. Electroanal. Chem.* **1990**, *296*, 371–394.
83. Engblom, S.O. *J. Electroanal. Chem.* **1992**, *332*, 73–99.
84. Engblom, S.O. *Anal. Chem.* **1992**, *64*, 2530–2538.
85. Baranski, A.S.; Lu, W. *J. Electroanal. Chem.* **1989**, *260*, 1–13.
86. de Levie, R.; Sarangapani, S.; Czekaj, P.; Benke, G. *Anal. Chem.* **1978**, *50*, 110–115.
87. Lavagnini, I.; Pastore, P.; Magno, F. *Anal. Chim. Acta* **1990**, *239*, 95–106.
88. Sybrandt, L.B.; Perone, S.P. *Anal. Chem.* **1971**, *43*, 382–388.
89. Sybrandt, L.B.; Perone, S.P. *Anal. Chem.* **1972**, *44*, 2331–2339.
90. Ichise, M.; Yamagishi, H.; Kojima, T. *J. Electroanal. Chem.* **1980**, *113*, 41–49.
91. Thomas, Q.V.; Perone, S.P. *Anal. Chem.* **1977**, *49*, 1369–1375.
92. Thomas, Q.V.; DePalma, R.A.; Perone, A.P. *Anal. Chem.* **1977**, *49*, 1376–1380.
93. DePalma, R.A.; Perone, S.P. *Anal. Chem.* **1979**, *51*, 825–828.
94. DePalma, R.A.; Perone, S.P. *Anal. Chem.* **1979**, *51*, 829–832.
95. Ichise, M.; Yamagishi, H.; Kojima, T. *J. Electroanal. Chem.* **1978**, *94*, 187–199.
96. Ichise, M.; Yamagishi, H.; Kojima, T. *J. Electroanal. Chem.* **1980**, *106*, 35–45.
97. Ichise, M.; Yamagishi, H.; Kojima, T. *J. Electroanal. Chem.* **1980**, *108*, 213–222.
98. Ichise, M.; Yamagishi, H.; Kojima, T. *J. Electroanal. Chem.* **1982**, *132*, 85–97.
99. Ichise, M.; Kojima, T.; Yamagishi, H. *J. Electroanal. Chem.* **1983**, *147*, 97–105.
100. Schachterle, S.D.; Perone, S.P. *Anal. Chem.* **1981**, *53*, 1672–1678.
101. Byers, W.A.; Perone, S.P. *Anal. Chem.* **1983**, *55*, 615–620.
102. Byers, W.A.; Freiser, B.S.; Perone, S.P. *Anal. Chem.* **1983**, *55*, 620–625.
103. Rusling, J.F. *Anal. Chem.* **1983**, *55*, 1713–1718.
104. Rusling, J.F. *Anal. Chem.* **1983**, *55*, 1719–1723.
105. Rusling, J.F.; Connors, T. F. *Anal. Chem.* **1983**, *55*, 776–781.
106. Palys, M.; Bos, M.; van der Linden, W.E. *Anal. Chim. Acta* **1990**, *231*, 59–67.
107. Palys, M.; Bos, M.; van der Linden, W.E. *Anal. Chim. Acta* **1991**, *248*, 429–439.